CR-116779

SYNTHESIS OF FEEDBACK SYSTEMS WITH LARGE PLANT IGNORANCE FOR PRESCRIBED TIME DOMAIN TOLERANCES

by

ISAAC M. HOROWITZ
MARCEL SIDI

This research was sponsored by the National Aeronautics and Space Administration under Research Grant NGR 06-003-083.

DEPARTMENT OF ELECTRICAL ENGINEERING
UNIVERSITY OF COLORADO
BOULDER, COLORADO

July 1, 1971

SYNTHESIS OF FEEDBACK SYSTEMS WITH LARGE PLANT IGNORANCE FOR PRESCRIBED TIME DOMAIN TOLERANCES

by

Isaac M. Horowitz

Marcel Sidi

This research was sponsored by the National Aeronautics and Space Administration under Research Grant NGR 06-003-083.

Department of Electrical Engineering
University of Colorado
Boulder, Colorado
July 1, 1971

TABLE OF CONTENTS

SYNTHESIS OF FEEDBACK SYSTEMS WITH LARGE PLANT IGNORANCE FOR PRESCRIBED TIME DOMAIN TOLERANCES

ABSTRACT

There is given a minimum-phase plant transfer function, with prescribed bounds on its parameter values. The plant is imbedded in a two-degree-of freedom feedback system, which is to be designed such that the system time response to a deterministic input lies within specified boundaries. Subject to the above, the design should be such as to minimize the effect of sensor noise at the input to the plant. This report presents a design procesure for this purpose, based on frequency response concepts. The time-domain tolerances are translated into equivalent frequency response tolerances. The latter lead to bounds on the loop transmission function $L(j\omega)$, in the form of continuous curves on the Nichols chart. The properties of $L(j\omega)$ which satisfy these bounds with minimum effect of sensor noise, are derived. The design procedure is very transparent, providing the designer with the insight to make any necessary tradeoffs, at every step in the design process. The same design philosophy may be used to attenuate the effect of disturbances on plants with parameter ignorance.

CHAPTER I

STATEMENT OF THE PROBLEM

1.1 Introduction

This report is devoted to the following problem. There is a single input-output 'plant' imbedded in a linear 'two-degree-of-freedom feedback structure'. The term 'plant' denotes the constrained part of the system, whose output is the system output. The designation 'two-degree-of-freedom feedback structure' indicates a system wherein the command input, $r(t)$ in Fig. 1.1, and the system output $c(t)$, may be independently measured. In such a structure[1] the system response to command inputs, and the system sensitivity to the plant may be, to some extent[2], independently controlled. The structure shown in Fig. 1.1 is of course only one of many possible canonic[1] two-degree-of-freedom feedback structures. The plant parameters are not known precisely. Only the ranges of their values are known. For example, the plant transfer function may be a known function of elements of the set $X = \{x_1, x_2, \ldots x_n\}$ but these elements are known only to lie in a given closed region in n-dimensional space. Clearly, the 'bounded ignorance' of the plant may appear in many different forms. Strictly speaking, the design technique is applicable only to fixed parameter plants, but it is well-known that for engineering purposes, it is also applicable to 'slowly-varying' plant parameters. It is much less known that the feedback is quite effective even for rather fast-varying plants[3]. However, this is a topic requiring considerable separate treatment, so it will be assumed in this report that the plant is fixed but there is on the designer's part ignorance, in the sense previously described, of the plant parameters.

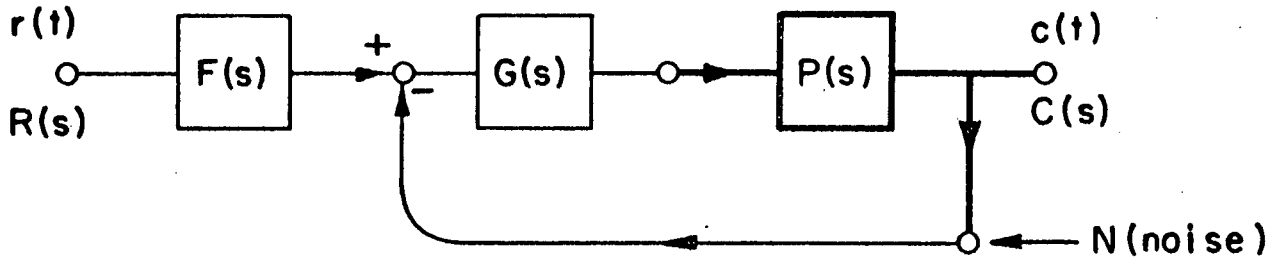

Fig. 1.1: A canonic two-degree-of-freedom feedback structure. (Darker portion is constrained part.)

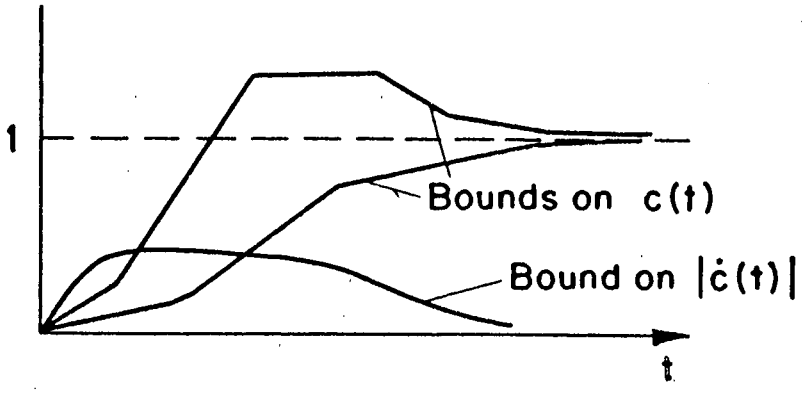

Fig. 1.2: Example of tolerances on unit step response.

The system sensitivity to the 'plant ignorance' is to be characterized by the resulting ignorance in the system time response to a specific deterministic time input. A unit step is chosen for the latter in this report, but any other input may be chosen for that purpose. The problem is to guarantee that the output ignorance is contained within prescribed bounds, for example, those shown in Fig. 1.2, for the case $r(t) = u(t)$, the unit step function. It is, of course, up to someone somewhere in the hierarchy, to provide these bounds. This report is concerned only with the means to satisfy such specifications. It can be shown[2] that if the plant is minimum-phase, then any such specifications, no matter how narrow the tolerances, may be approached as closely as desired. From this, it follows that it is easy to over-design in minimum-phase systems. The 'price' paid in general is in the large 'bandwidth' of the loop-transmission function, with transfer function $L(s)$, which in turn opens wider the 'window' to the noise in the feedback return path, lumped as sensor noise N in Fig. 1.1 . In the high-frequency range where $|L(j\omega)| < 1$, but where $|P(j\omega)| < |L(j\omega)|$, the noise is amplified by $|L(j\omega)/P(j\omega)|$, which tends to be very large over a large bandwidth, in such systems. The amplified noise tends to saturate the output stages of $G(s)$ or input stages of $P(s)$. This problem has been emphasized before[4] .

1.2 Optimization Criteria

This report copes with the above problem by taking the response bounds as inviolate, but attempting to satisfy them with an $L(j\omega)$ whose magnitude as a function of frequency is decreased as fast as possible. This decreases the effect of the sensor noise, if it is strong in the relatively higher frequency range. Another approach would be to minimize an index into which enter both the spread in the response and

the effect of the noise. Statistical methods have been very useful for such indices, for many problems in which the plant parameters are precisely known. Attempts to do the same for the present problem have been unsuccessful because of the need to obtain expectations over P of expressions like $P/(1+PM)$. The practice[5] has been to neglect the ignorance of P in the denominator, and replace it there by some nominal P_0 , but this is obviously a very poor approximation for plants with significant ignorance bounds. The optimization criterion used in this report is discussed further in Section 3.1 .

1.3 Previous Work

There have been two principal approaches to the problem considered in this report, under the constraint of linear, fixed compensation functions G,F in Fig. 1.1 . (This constraint eliminates the class of nonlinear feedback, or nonlinear 'adaptive' systems.) One approach is that of the dominant pole-zero method[6,7,8] which has been reasonably well documented. The other approach has been by the frequency-response method, of which this report is the most recent contribution. The philosophy of the frequency-response method is to translate the system time-domain bounds into equivalent bounds on the magnitude (and/or phase) of system transfer function frequency response. This first step remains to this day nonrigorous and approximate. The second step is to translate these frequency response bounds into equivalent ones on the loop transmission function, $L(s) = GP$ of Fig. 1.1 . In previous work the method used was based on the equation[9,10,11]

$$\frac{T(j\omega)}{T_0(j\omega)} = \frac{1 + L_0(j\omega)}{\frac{P_0(j\omega)}{P} + L_0(j\omega)} \tag{1.1}$$

where P_0 is the nominal plant function at which the system transfer function has its nominal value, T_0 . When the

plant function is P , the corresponding system function is T . L_0 is the nominal value of the LTF, i.e., $L_0 = GP_0$. From Equation (1.1), given the range of $\frac{P_0}{P}(j\omega)$, it is straightforward to find the bounds on $L_0(j\omega)$, at any ω , such that the bounds on T_0/T are not violated. These bounds on $L_0(j\omega)$ are obtained at as many discrete frequencies as one may wish. The third step is to choose a satisfactory $L_0(j\omega)$, such that the above bounds on L_0 are satisfied. This determines $G = L_0/P_0$, and then F is chosen from the relation

$$T_0 = F\, L_0/(1+L_0) \ .$$

This design technique has remained virtually unchanged since 1959 when it was first presented. It has three distinct shortcomings: (1) the nonrigorous, approximate nature of step 1, in which time-domain bounds are translated into equivalent frequency-response bounds. (2) the need in the second step to make at the outset a pairing of a nominal response function with a nominal plant function. An experienced designer can usually make a reasonable good pairing. Normally, the slowest admissible response function corresponds approximately to the slowest, smallest magnitude plant. However, even the very experienced designer has very small probability of a priori choosing a pairing which proves to be optimal. And the inexperienced designer may initially make a very poor pairing and be forced to a second round. This specific shortcoming disappears in the revised method presented in this report, by eliminating entirely the need for pairing. Finally, the third shortcoming is in the lack of guide-lines for the third step, i.e., finding the optimum $L_0(j\omega)$ which does satisfy the set of bounds derived in step 2. This shortcoming is very significantly reduced in the present work, in which there are presented many of the properties of the ideal $L(j\omega)$.

CHAPTER 2

DERIVATION OF BOUNDS ON $L(j\omega)$

2.1 Templates of $P(j\omega)$

It is assumed that the translation of time-domain into frequency-domain specifications has been accomplished and the latter are of the form shown in Fig. 2.1. For example, at $\omega = 5$ rps, $|C(j5)|$ is permitted to be anywhere between -2.5 and -13.5 db ; $|C(j10)|$ between - 7.0 and - 27.0 db , etc. Since $C = RT = RFL/(1+L)$ and there is no ignorance of F, G ,

$$\Delta\ell n|C(j\omega)| = \Delta\ell n|T(j\omega)| = \Delta\ell n\left|\frac{L(j\omega)}{1+L(j\omega)}\right| \tag{2.1}$$

with

$$L = GP \quad \text{(see Fig. 2.2)}$$

$$\Delta\ell nL = \Delta\ell nP \ . \tag{2.2}$$

A specific value of frequency is chosen; say $\omega = \omega_1$ rps . The values of $P(j\omega_1)$ over the range of plant parameters are calculated and the bounds obtained. The procedure is illustrated for the case

$$P(s) = \frac{ka}{s(s+a)} \ ; \quad 1 \leq k \leq 10 \ ; \quad 1 \leq a \leq 10 \ . \tag{2.3}$$

This is done on the plane of $\ell n\, L\,(j\omega) = \ell n|L| + j\ \text{Arg}\ L$, the abscissa in degrees and the ordinate in decibels (the Nichols chart). Thus, at $\omega = 2$ rps, $P(2j)$ lies within the boundaries given by ABCD in Fig. 2.3. Since $\ell n\, L = \ell nG + \ell nP$, the pattern outlined by ABCD may be translated (but not rotated) on the Nichols chart, the amount of translation being given by the value of $G(2j)$. For example, if a trial design of $L(2j)$ corresponds to

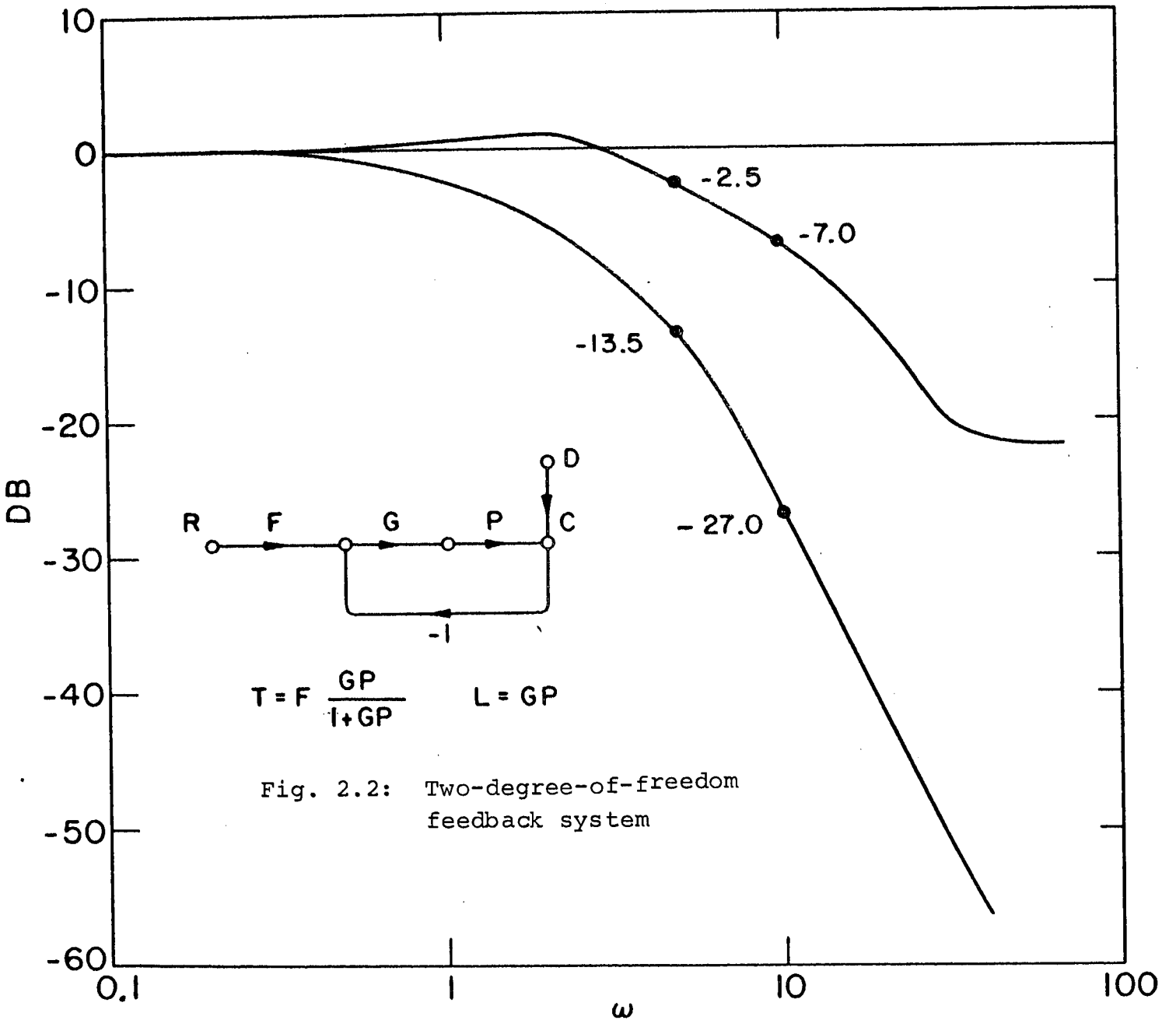

Fig. 2.2: Two-degree-of-freedom feedback system

Fig. 2.1: Bounds on $|T(j\omega)|$

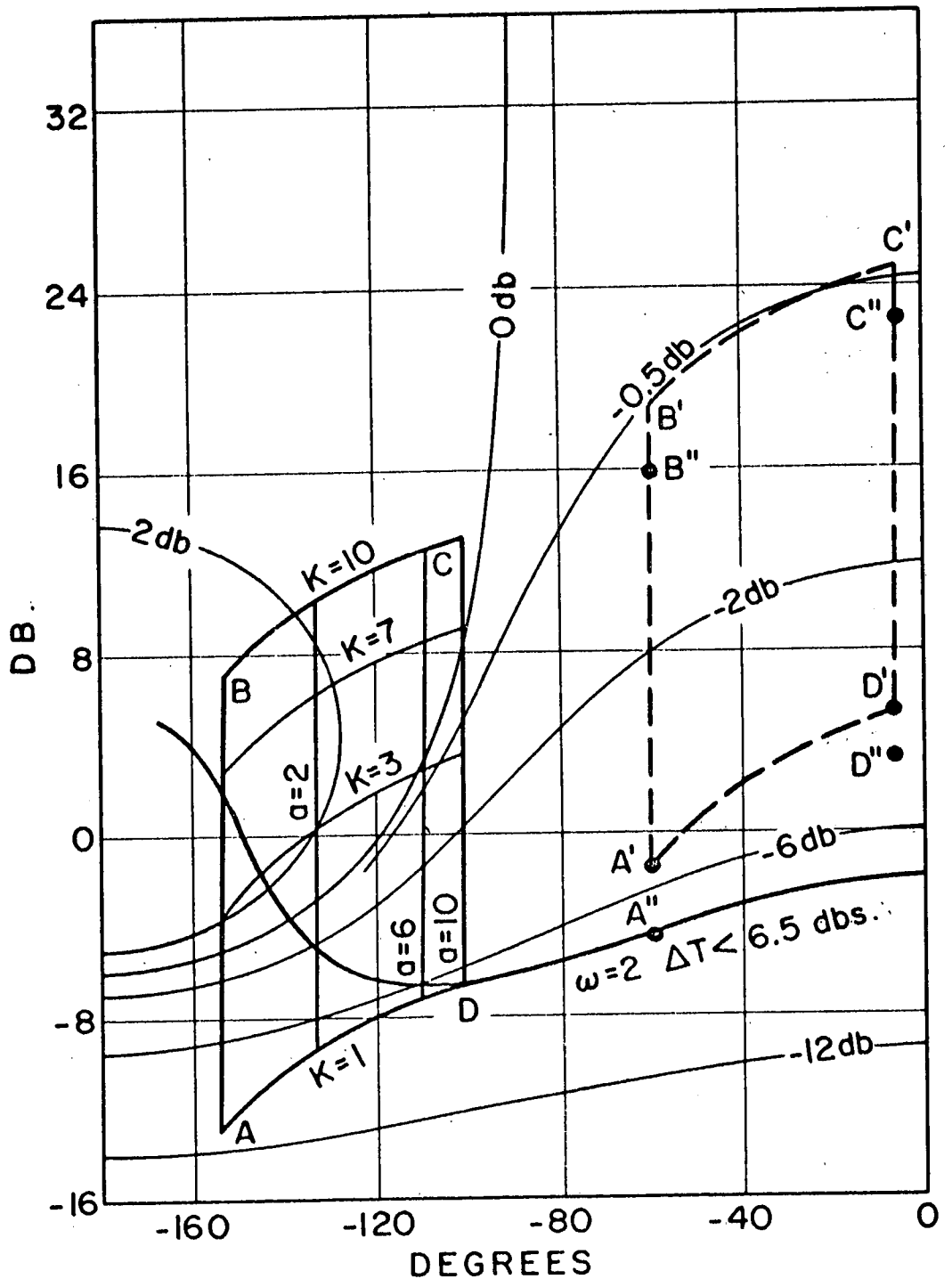

Fig. 2.3: Range of P(j2) and resulting bounds on L(j2), on Nichols Chart

the template of $P(2j)$ being translated to the new position A'B'C'D' in Fig. 2.3, then

$|G(2j)| = |L(2j)| - |P(2j)| = (-2.0) - (-13.0) = 11.0$ DB ;

$\text{Arg } G(2j) = \text{Arg } L(2j) - \text{Arg } P(2j) = (-60°) - (-153.4°) = 93.4°$.

2.2 Bounds on $L(j\omega)$ in the Nichols Chart

The templates of $P(j\omega)$ are manipulated to find the position of $L(j\omega)$ which results in the specifications of Fig. 2.1 on $\ell n|T(j\omega)|$ being satisfied. Taking the $\omega = 2$ template, one tries, for example, positioning it, as shown in Fig. 2.3, at A'B'C'D' . Contours of constant $\ell n|L/(1+L)|$ are available on the Nichols chart. Using these contours it is seen that the maximum change in $\ell n|L/(1+L)|$ which, from Equation 2.1, is the maximum change in $\ell n|T|$ is, in this case, very closely $(-0.49) - (-5.7) = 5.2$ DB, the maximum being at the point C' , the minimum at the point A' . The specifications of Fig. 2.1 tolerate a change of 6.5 DB, at $\omega = 2$ so $|L(j2)|$ is in this case more than satisfactory. One may shift the template lower on the Nichols chart, until the bounds on $\Delta\ell n|T|$ correspond to 6.5 D.B. This is achieved when the lower left corner of the template is at A'' in Fig. 2.3 . The template corners are at A''B''C''D'' and the extreme values of $\ell n|L/(1+L)|$ are at C'' (-0.7 DB), A'' (-7.2 DB) . If $L(2j)$ for condition A is chosen to be -4.2 DB $\angle -60°$, then it is guaranteed that $\Delta\ell n|T(j)| \leq 6.5$ DB, over the entire range of plant parameter values. If $\text{Arg. } L_A(2j) = -60°$, then -4.2 DB is the smallest magnitude of $L_A(2j)$ which satisfies the 3.2 DB specification for $\Delta\ell n|T|$. Any larger magnitude is satisfactory but represents, of course, overdesign at that frequency.

The manipulation of the $\omega = 2$ template may be repeated along a new vertical line, and a corresponding new minimum of $|L_A(2j)|$ found. Sufficient points are obtained in this manner to permit drawing a continuous curve of the bound on

$L_A(2j)$, as shown in Fig. 2.3 . The entire process may be repeated at other frequencies. Fig. 2.4 shows the outline of the templates and the resulting bounds on $L_A(j\omega)$, for a number of frequencies. The template outlines are drawn at any available convenient areas on the Nichols chart, since they are, in any case, translated later. In each case the permissible region is to the right of the curve. It is important to note that although condition A (a=k=1) was chosen to generate the curves, any other set of values of a, k could have been chosen. However, once condition A was chosen at any one value of ω , this same condition A must be used for all the contours. If the bounds on L_A are satisfied, then automatically those on all other sets of parameter values, as encompassed by the templates, are also satisfied. This means that $\Delta\ell n|T(j\omega)|$ will not exceed the specifications of Fig. 2.1 .

Since $P(s)$ is infinite at $\omega = 0$, the system is Type 1, and the zero frequency specification on $\Delta\ell n|T|$ (assuming it is zero) can be satisfied with any finite value for $\lim_{s\to 0} sL(s)$. In practice there will be a requirement on the velocity constant which will give a lower bound on $\lim_{s\to 0} sL(s)$.

2.3 System Response to Disturbances

The system response to command inputs $r(t)$ (of Fig. 2.2) is not the only response function of interest. There are, in most systems, also disturbances to be considered. The disturbance response (for D in Fig. 2.2), is

$$C_D(s) = \frac{D(s)}{1+L(s)} \tag{2.4}$$

It is necessary, of course, to choose $L(s)$ so that the disturbances are properly attenuated, and the technique of

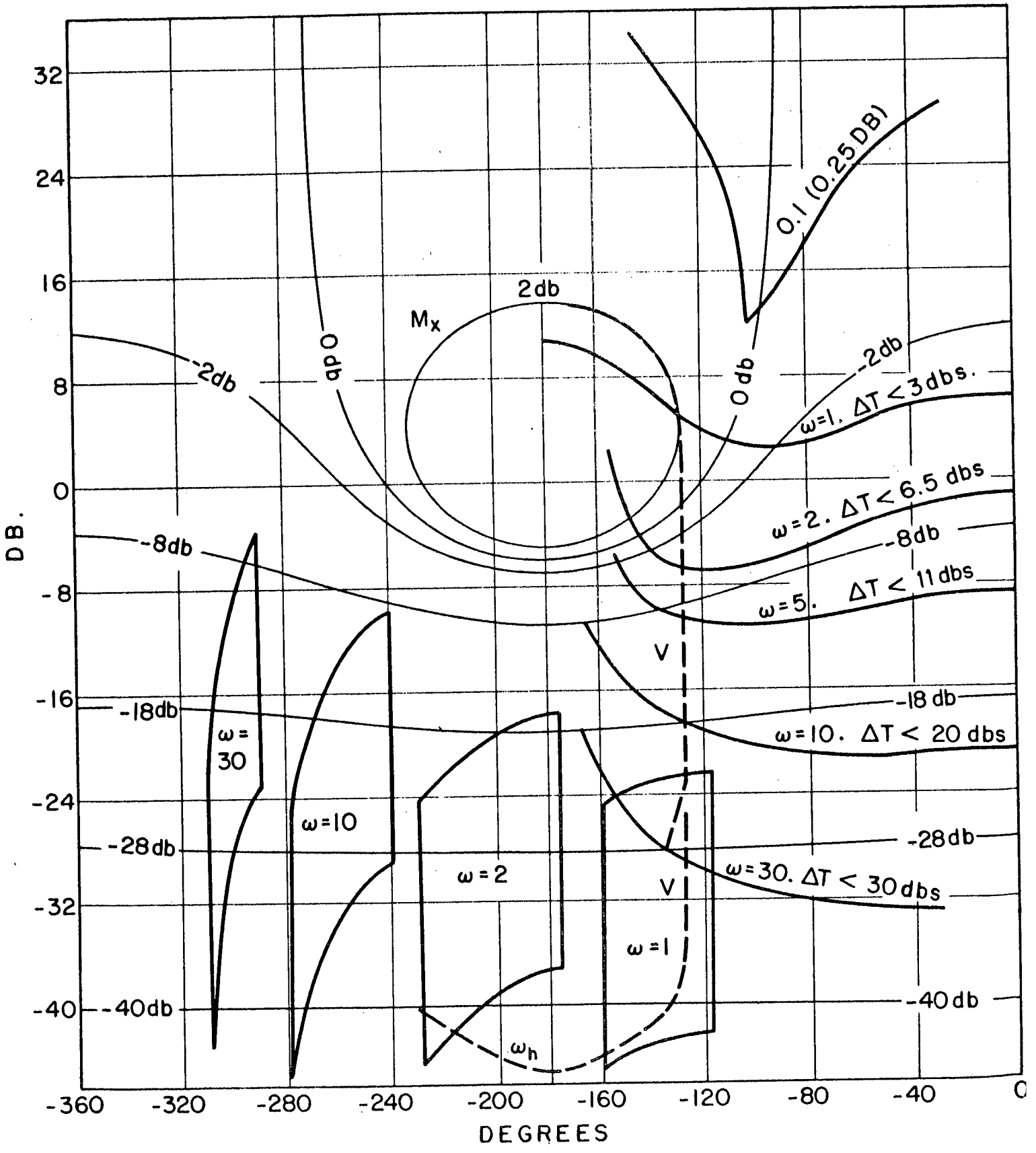

Fig. 2.4: Boundaries of $L(j\omega)$ on the Nichols Chart

this report lends itself very readily for this purpose, as detailed in Section 7.2 . For the present, only one aspect of this disturbance response problem will be considered, namely, that there will generally be a constraint on the damping factor of the pole pair nearest the $j\omega$ axis. This damping factor can be related to the peaking in

$$\left| \frac{L(j\omega)}{1+L(j\omega)} \right| \quad .$$

Thus, using the single complex pole pair as a model, a peak of 8 db corresponds closely to a damping factor $\zeta = 0.2$; 2.7 db to $\zeta = 0.4$, etc. The usual constraint on the damping factor can therefore be translated into a constraint on the peak value of $|L/(1+L)|$. Suppose this happens to be 2 db, in the present example. If so, the contours in Fig. 2.4 must be modified, as they now permit peaking greater than 2 db . The required modifications are shown by the dashed lines. The parts of the contours rendered invalid because of the above requirement are to the left of the dashed lines. Note that a portion of the $|T| = 2$ db locus is common to all the contours.

2.4 The single high-frequency boundary

At large frequencies, $\omega >> a_{max} = 10$

$$P(j\omega) \rightarrow \frac{ka}{(j\omega)^2}$$

and the template becomes a vertical line of length $|\Delta ka|_{max}$, which is 40 db. At these frequencies, from Fig. 2.1, it is seen than $\Delta \ell n|T|$ is allowed to be more than 40 db . Hence, the only constraint on $L(j\omega)$, for the higher frequency range, is that $|L/(1+L)| \leq 2$ DB , due to disturbance response. This gives the contour marked ω_h , in Fig. 2,4, which will be valid for all frequencies higher than ω_h , with $\omega_h \simeq 5a_{max}$.

A reasonable number of discrete frequencies must be worked out in the above manner to ensure that, at the frequencies omitted, the design will also be satisfactory. The next step is to choose the optimum $L(j\omega)$ which satisfies the above bounds. Important properties of the optimum $L(j\omega)$ are derived in the following two chapters.

CHAPTER 3

PROPERTIES OF OPTIMUM $L(j\omega)$ - NECESSARY AND SUFFICIENT CONDITIONS FOR BOUNDARIES OF NEGATIVE SLOPE

3.1 Definition of Optimum $L(j\omega)$ and its Justification

This chapter is devoted to the derivation of the optimum $L(j\omega)$ function, which is defined as follows. At very high frequencies

$$L(j\omega) \to \frac{K}{(j\omega)^e} \quad , \tag{3.1}$$

where e is the excess of poles over zeros of $L(s)$. The optimum $L(j\omega)$ is the one which satisfies the specifications, as obtained in Chapter 2, and whose K, of Equation (3.1), has the minimum possible value. What is the reason for this definition of optimum? It lies in the effect of noise in the feedback loop on design practicality.

In Fig. 3.1, Φ_N represents the power spectrum of sensor and amplifier noise, referred to an indicated point in the loop. A typical difficult adaptive problem, i.e., one with relatively large ignorance or narrow response bounds, will require relatively large $|L|$ over a large bandwidth. The principal reason is the existence of an almost vertical boundary line, extending over a large range, like the one with phase of -127°, in the specific example of Fig. 2.4 . This line is a boundary of permissible $L(j\omega)$ over a large frequency range. It extends vertically for approximately 40 db, because the range of K of Equation (3.1) is precisely 40 db (recall $K = ka$ in the example of Chapter 2 with $1 \leq k, a \leq 10$) . The phase lag of $L_A(j\omega)$, [recall A corresponds to the condition $a = k = 1$], must not exceed 127°

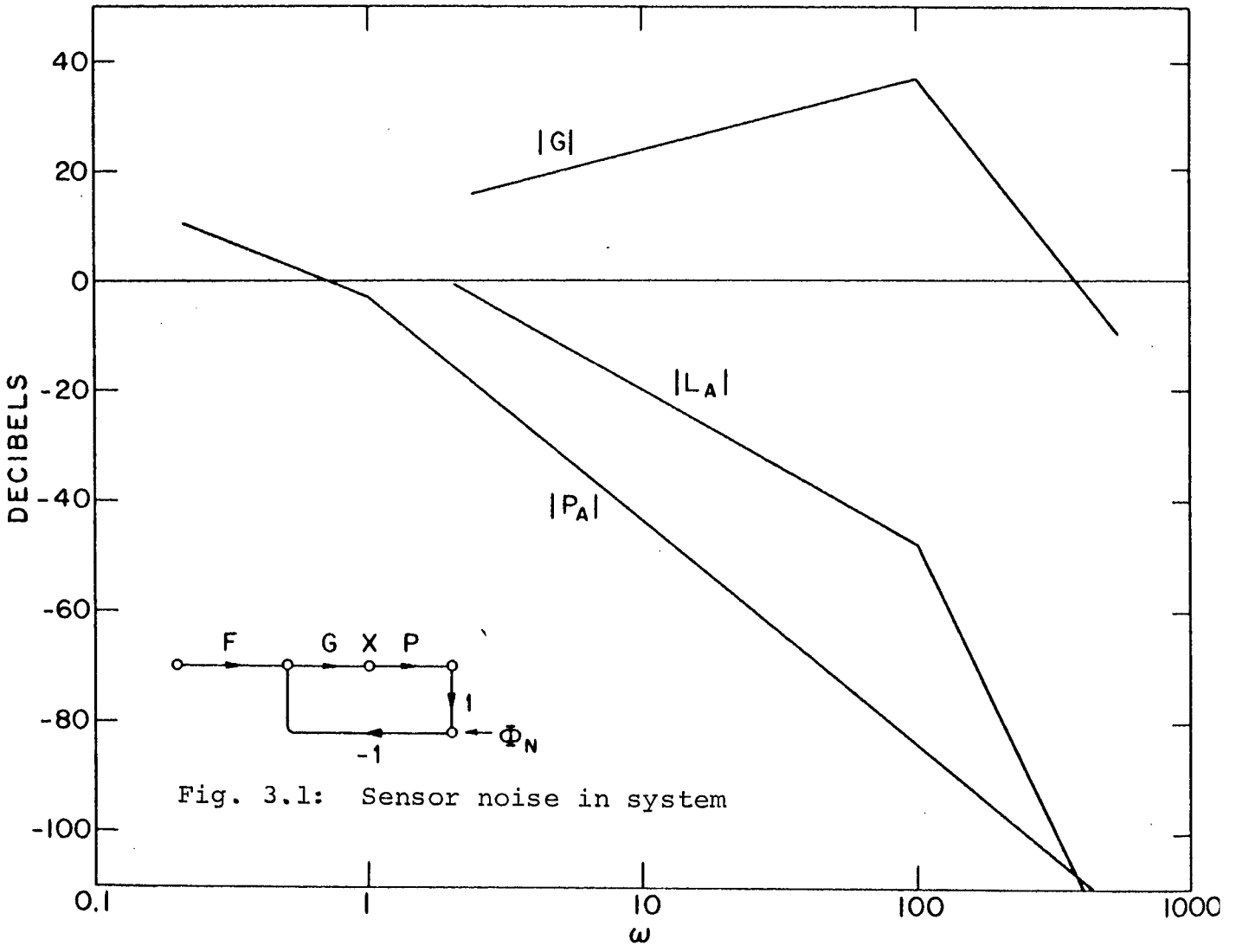

Fig. 3.1: Sensor noise in system

Fig. 3.2: Principal factors in sensor noise problem

for $\omega < \omega_h \approx 50$ rps. In Fig. 2.4, at $\omega = 5$, $|L_A|$ can be approximately - 11 DB . Let us assume $L_A(j\omega)$ has the maximum allowable lag of 127° for $\omega > 5$ up to $\omega = 50$. Then the average slope of $|L_A|$ over this decade is $-(127/180)40 = -28.2$ DB per decade. Hence, at best, $|L_A(j50)| \approx -11 -28.2 = -39.2$ DB . If the bounds for the frequencies between 5 and 50 rps do not interfere, it appears feasible to have $|L_A(j50)| \approx -40$ DB . Note, however, that if the range of k happened to be, say, 100 instead of 10, then the range of K would be 60 DB and the vertical line would extend down to approximately -60 DB, while the boundaries at $\omega = 5,10,30$ would be basically unchanged. In such a case, $|L_A|$, would have to decrease at this 'slow' rate of -28.2 DB per decade until $|L_A| \approx -60$ DB, which would require $60/28.2 = 2.1$ decades beyond $\omega = 5$, i.e., up to $\omega = \omega_x = (5)\ 10^{2.1}$. The phase lag of L_A may be sharply increased only after $\omega > \omega_x$, permitting only then a much faster reduction of $|L_A|$. Essentially, it is a matter of gain margin. If the range of K is 100 , a gain margin > 40 DB is required, etc.

In Fig. 3.1, the effect of the noise at X is obtainable from the power spectrum of X_N , denoted by

$$\Phi_{XN} = \Phi_N \left| \frac{G}{1+L} \right|^2 = \Phi_N \left| \frac{L/P}{1+L} \right|^2 . \qquad (3.2)$$

using the relation

$$(x_N)_{RMS} = \{ \int_0^\infty \Phi_{XN}\, d\omega \}^{1/2} . \qquad (3.3)$$

The principal factors in the noise problem can be explained with the aid of Fig. 3.2, in which a hypothetical design example is presented, $|L_A(j5)| \approx -11$ DB and decreases at the rate of -28.2 DB per decade up to 100 RPS at which it is generously assumed that the slope can be instantaneously

changed to -100 DB per decade. $|P_A(j\omega)|$ is also shown, and so is $|G| = |L_A/P_A|$. In the frequency range where $|L_A| << 1$, $|1+L_A| \approx 1$, and $|L_A| < 1$ for $\omega > 40$ which, from Fig. 3.3, is the most significant range for calculating $(x_N)_{RMS}$. Thus, in this important frequency range

$$\Phi_{XN} \approx \Phi_N |L/P|^2 = \Phi_N |G|^2 . \qquad (3.4)$$

Since P is beyond the designer's control, it is most important to reduce $|L|$ as quickly as possible, as a function of frequency. Hence, the importance of having tolerances as large as possible for $\Delta \ell n|T|$, and for optimizing $L_A(j\omega)$, in the sense indicated. It is important to note that arithmetic scales are used in Fig. 3.3 for finding $(x_N)_{RMS}$. Hence the saving of even a few db or of a part of an octave in $L(j\omega)$ has a significant effect on x_N.

The definition of optimum $L(j\omega)$, [minimum K of Equation 3.1], is reasonable when the noise is white. But if this is not so, for example, if there is a sharp peaking of the noise, say at $\omega = 10$, in the example of 2.4, then it would appear that a more precise definition of optimum directly in terms of Φ_N etc. would be necessary, leading to emphasis in the 10 rps range where Φ_N is unusually large. Note, however, that in any case such a redefinition would not help matters much, as the bound on $L(j10)$ in Fig. 2.4 precludes drastic reduction of $|L(j10)|$. (In fact, it is not an unreasonable conjecture that the definition of optimum L being used leads to the minimization of $|L|$ at every frequency, but this is only a conjecture.) Hence, significant reduction of $|L(j10)|$ requires a significantly lower boundary on the Nichols chart of $L(j10)$, which would, of course, affect the time domain response for some combinations of plant parameter values. This is now

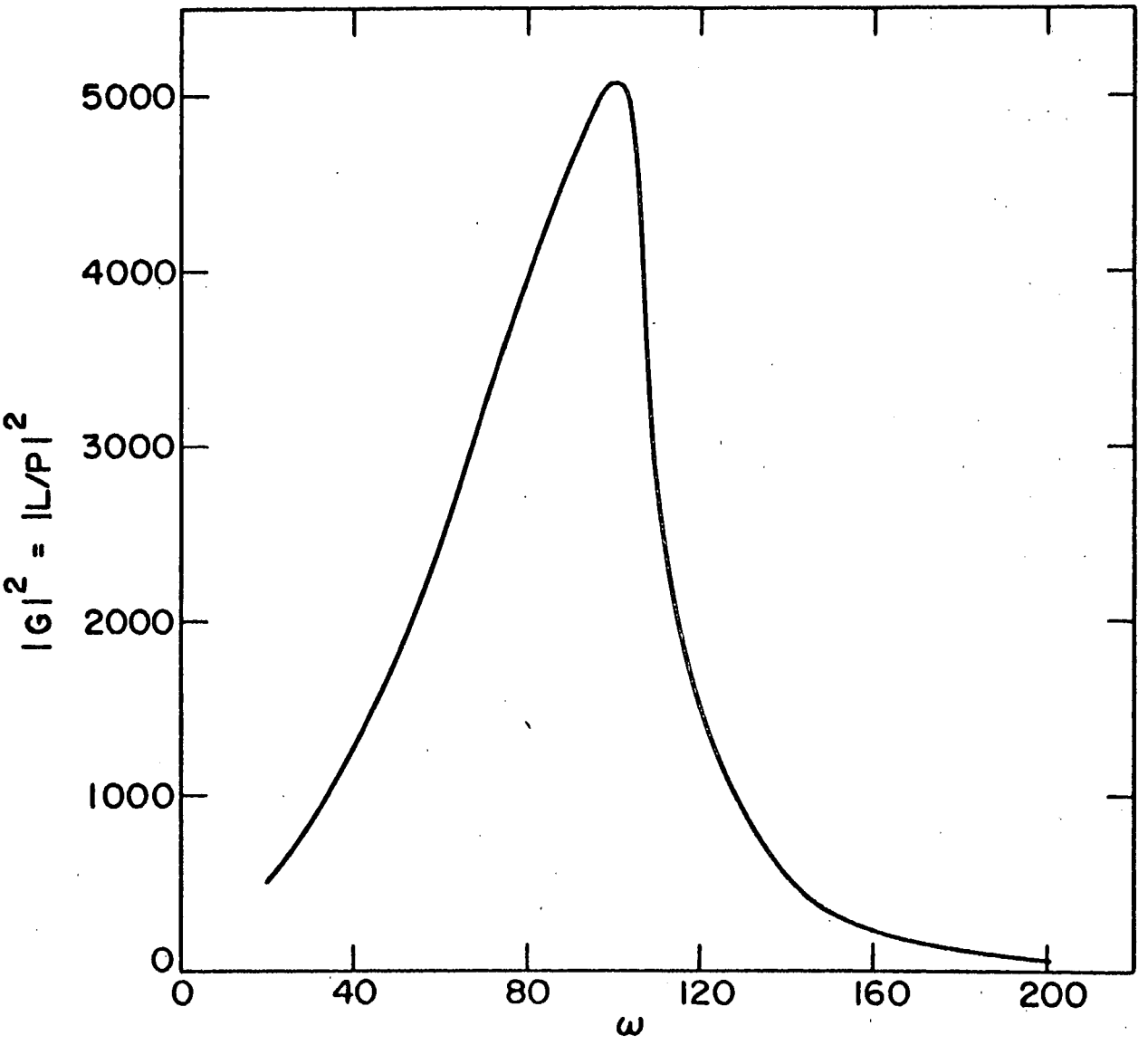

Fig. 3.3: Calculation of $(x_N)_{rms}$

a matter of compromise between the time domain specifications and the noise response, and would have to be handled at that level. Of course, an optimality criterion which includes within it both these factors would therefore be superior in this respect. But, as noted in Chapter 1, there has been no success in applying such a criterion to this problem.

Estimate of $L(j\omega)$. An excellent idea of how fast $|L_A(j\omega)|$ may be decreased is obtainable from a simple physical inspection of the L_A contours of Fig. 2.4 . It is of course desirable that L_A have as large a lag angle as possible because the phase is, in a general sense[13] proportional to $\frac{d\ell n|L|}{d\ell n\omega}$. Since the boundaries tend to increase with phase lag (at least on the left side which is the desirable larger phase lag side), there will be a compromise. If the slopes of the boundaries are rather gentle, as they are for those in Fig. 2.4, then the optimum L_A will probably pass through points near the minima on the boundaries. There is also the matter of consistency, of the slope of $|L_A|$ with the location of the contours. For example, if $L_A(j2)$ is chosen ≈ -6.5 DB $\angle -127°$ and it has this lag angle over an octave or so, then the rate of decrease of $|L_A|$ near $\omega = 2$ is approximately $(127/180)12 = 8.5$ db per octave. Hence at $\omega = 5$, which is 1.32 octaves away, $|L_A|$ will be approximately $-6.5 - 1.32(8.5) = -17.7$ db, which is well below the boundary for $\omega = 5$. The optimum L_A will therefore probably have less than the above phase lag at $\omega = 2$. It is seen that the problem is not an easy one.

3.2 Derivation of Optimum $L(j\omega)$ for negative slope boundaries-necessary conditions

A boundary curve on the Nichols chart (for example, as in Fig. 2.4) can be written as $|F| = f(\theta)$. It is assumed in this chapter that $d|F|/d\theta$ is negative over the entire range.

This is generally the situation at larger frequencies, but isn't so at the lower frequencies (see Fig. 2.4) . However, it has been noted that it is desirable to work in the larger phase lag region in which all the contours have the negative slope character. If the system is Type 1 or 2, then one may, in fact, be in this negative slope region for all, or almost all of the frequency range. This is not true for Type 0 systems where Arg $L(0) = 0°$, where $L(j\omega)$ must originate on the zero degreee vertical line and then, perforce, must cross a region where the contours tend to have positive slope. Nevertheless, we shall first assume the negative slope condition, because it is then possible to determine necessary and sufficient conditions for the ideal L (denoted as L_I) and prove that L_I exists and is unique. The more general case of boundaries of general V shape, is considered in Chapter 4.

The derivation of the optimum $L(j\omega)$ for the negative slope case, is accomplished in the following steps.

(1) Derivation of necessary conditions.

(2) Uniqueness of the function which satisfies the necessary conditions of Step 1, on the assumption of fixed $L(0)$ for Type 0 system, or fixed $\lim_{s\to 0} sL(s)$ for Type 1 system, etc. This is done in Sec. 3.3 .

(3) Proof that the optimum, if it exists, will have its $L(0)$ [or $\lim_{s\to 0} sL(s)$ etc.] at its minimum permissible value (Sec. 3.4).

(4) Proof of existence of optimum (Sec 3.5).

Taken together, the above provide necessary and sufficient conditions for the optimum $L(j\omega)$.

Step 1. Derivation of necessary conditions

Necessary conditions are derived by proving that any postulated $L_1(j\omega)$, which does not satisfy these conditions, can be improved by using instead

$$L_2(j\omega) = F(j\omega)L_1(j\omega)$$

which is "better" than $L_1(j\omega)$. For this purpose the three F (F_A, F_B, F_C) building blocks in Fig. 3.4a, b, c are useful. It can be assumed that the phase in Fig. 3.4a and the magnitude characteristics in Fig. 3.4 b,c are first chosen and then the missing characteristic is obtained from the Bode integral relations [14,15]. The important properties of these building blocks are indicated by the dashed vertical lines in Fig. 3.4, viz., for all ω to the left of XX' in Fig. 3.4a, $\angle F_A$ is zero, while $|F_A|_{DB} > 0$ etc. In Fig. 3.4a, note [15] that $\Delta = (2/\pi)$ times the shaded area of Fig. 3.4a.

Let M_x be the locus, on the Nichols chart, of the maximum $|L/(1+L)|$ allowed due to the peaking specifications on the disturbance response. Let V be the vertical line tangent to M_X, corresponding to the maximum phase lag allowable until the required gain margin is obtained to take care of $|\Delta K|$ (of Equation (3.1)). For example, V extends from 5 to - 36 DB in Fig. 2.4. Let ω_h be the smallest frequency for which V constitutes the right-hand part of the boundary of permissible $L(j\omega_h)$, i.e., for all $\omega \geq \omega_h$ the boundaries have no portions to the right of V ($\omega_h \approx 50$ in Fig. 2.4). It is generally the lowest frequency for which the permissible Δ& n$|T|$ exceeds the height of the P template. This usually occurs at a frequency sufficiently large such than the P template is almost a vertical line.

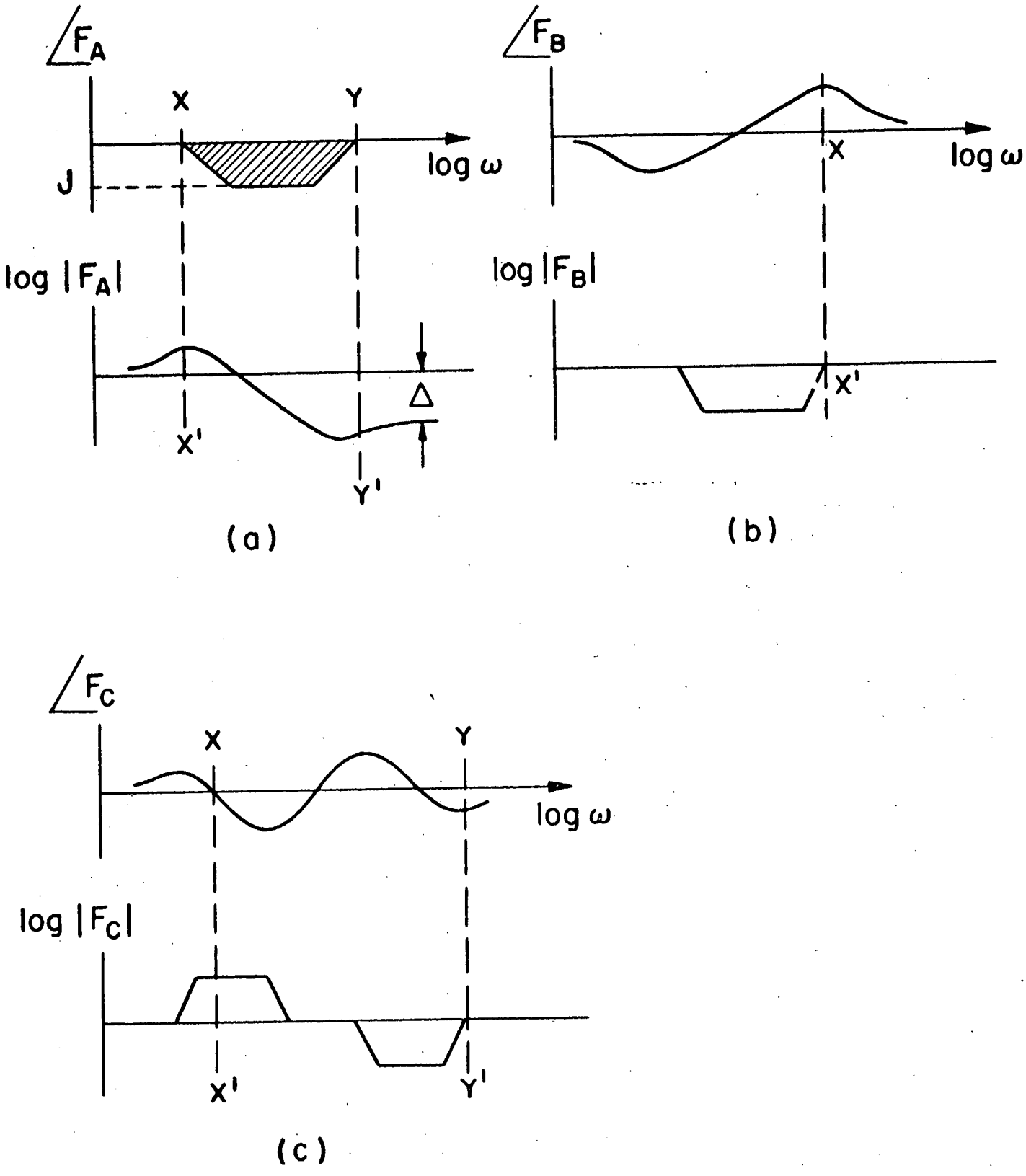

Fig. 3.4: The three building blocks

Necessary condition 1 (for boundaries of any slope)

For all $\omega \geq \omega_h$, the optimum $L(j\omega)$ will have no portion to the right of V .

Proof.

Suppose an $L_1(j\omega)$ is postulated which does not satisfy Condition 1, but for some frequency range $\omega_h \leq \omega_1 \leq \omega < \omega_2$, lies to the right of V , as in Fig. 3.5 . This means that L_1 for this range has less phase lag than that allowed. Let $L = F_A L_1$ with ω_1 on the line XX' in Fig. 3.4a, ω_2 on the line YY' . The arrows in Fig. 3.5 indicate the effect of F_A on L_1. For all $\omega < \omega_1$, $|L| \geq |L_1|$ at the same phase, so that L_1 certainly lies on or above the boundaries if L_1 does (see Fig. 3.5, where the dots denote L_1 positions and the arrows denote the general position of $L = F_A L_1$) . For $\omega_1 \leq \omega \leq \omega_2$, $\angle L < \angle L_1$, but this is tolerable. The level J of the building block of Fig. 3.4a need only be adjusted such that L does not cross the vertical line V . J is finite, even though it may be small. At high frequencies $|L| < |L_1|$ by a finite amount $\Delta = (2/\pi)$ times the shaded area of Fig. 3.4a . For all $\omega \geq \omega_2$ $\angle L = \angle L_1$, so the constraints on L for $\omega > \omega_2$ are still satisfied. Note that this necessary condition applies, whatever the slope of the boundaries, as the proof is valid for boundaries of any slope.

Necessary condition 2 (for boundaries of any slope)

The optimum $L(j\omega)$ must lie on the boundaries in the frequency range immediately below ω_h .

Proof

Again, let L_1 not satify this condition, in that for the range $\omega_x \leq \omega \leq \omega_h$ it lies above its boundaries (see Fig. 3.6) . Again, let $L = F_A L_1$, using building block A of Fig. 3.4a for F_A , with ω_x on XX' , ω_h on YY' .

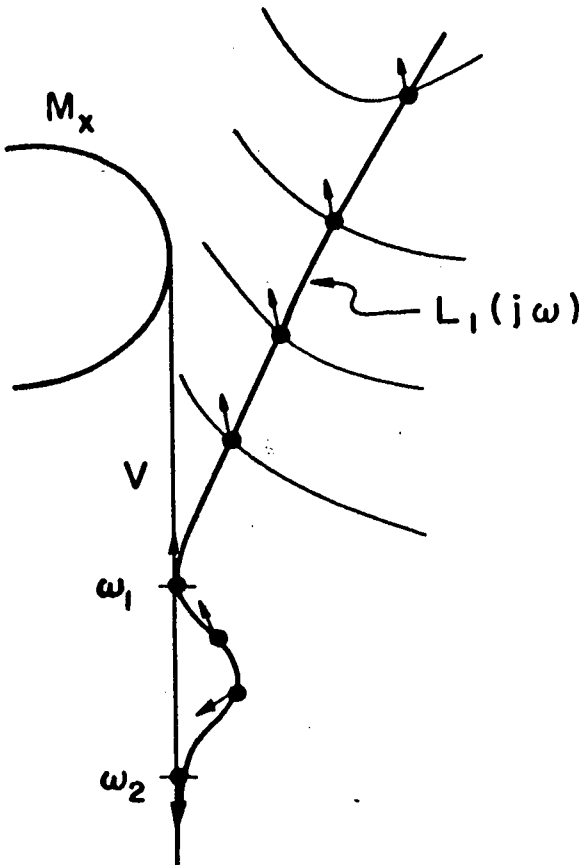

ig. 3.5: L_{OPT} must lie on V for $\omega \geq \omega_h$

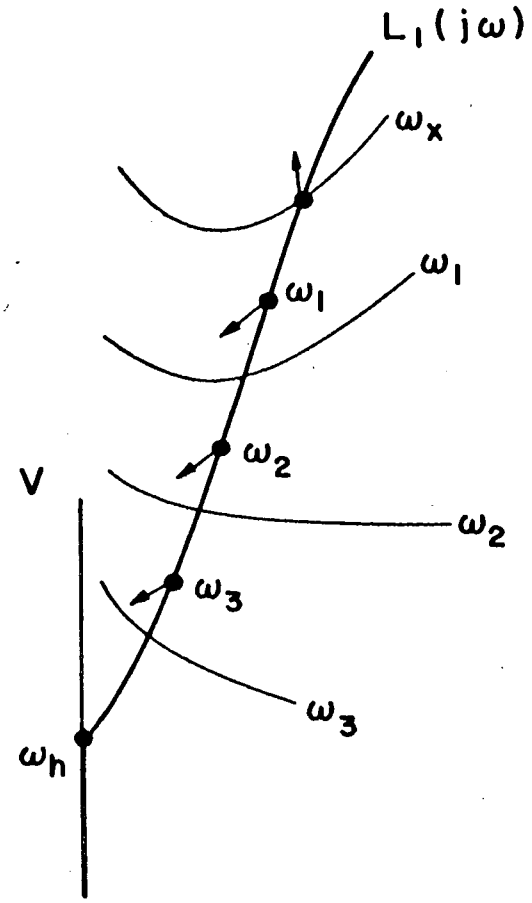

Fig. 3.6: Proof of necessary condition 2

The effect of F_A is indicated by the arrows in Fig. 3.6 . For all $\omega \leq \omega_x$, L certainly lies above the boundaries, if L_1 did. At high frequencies $|L| < |L_1|$ by the amount $\Delta = 2/\pi$ times the shaded area of Fig. 3.4a . Only in the range $\omega_x \leq \omega \leq h$ does L tend to be closer to the boundaries than L_1 , but the latter has a 'surplus' area in precisely this range. J may be adjusted until L lies precisely on a boundary at one or more $\omega_x \leq \omega \leq \omega_h$. Again, the proof is valid whatever the slopes of the boundaries.

Necessary condition 3. (only for boundaries of negative slope)

In the frequency range immediately above $\omega = 0$, the optimum L must lie on the boundaries.

Proof.

Assume L_1 does not lie on the boundaries for $0 < \omega < \omega_4$, (Fig. 3.7) . Let $L = F_B L_1$, F_B of the kind shown in Fig. 3.4b, with ω_4 on XX' . The effect is shown by the arrows in Fig. 3.7 . For all $\omega \geq \omega_4$ the new L lies above the boundaries, even if L_1 lay exactly on the boundaries for $\omega \geq \omega_4$. Hence, the techniques used for conditions 1, 2 may now be used to improve matters. Essentially, F_B permits the shifting of a "surplus" from the low frequency region, to a more convenient high-frequency region, where the techniques of conditions 1,2 may be used.

Necessary condition 4 (only for boundaries of negative slope)

The optimum L cannot have any range in which it lies above the boundaries.

Proof.

It has already been shown that the optimum L must lie on the boundaries above and immediately preceding ω_h , and for the range immediately following $\omega = 0$. Consider an L_1 which

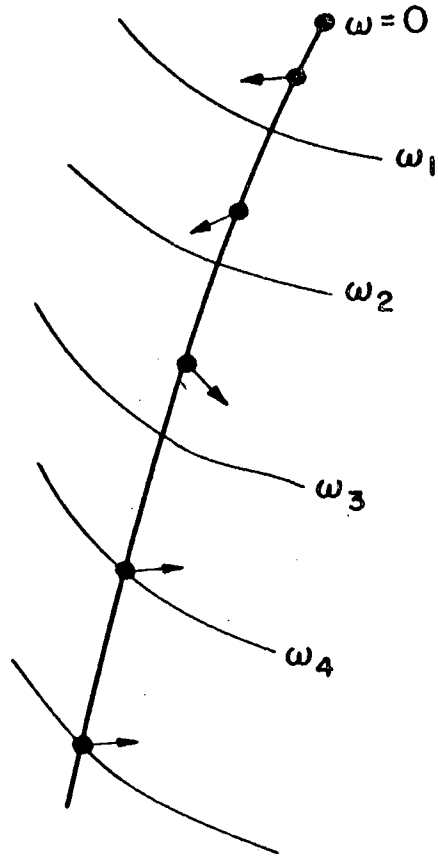

Fig. 3.7: Proof of necessary condition 3

lies above the boundaries for any range $\omega_A < \omega < \omega_B$ (Fig. 3.8) . Let $L = F_c L_1$, F_c of Fig. 3.4c with ω_A at XX' , ω_B at YY' . The arrows show the effect of F_c in Fig. 3.8. For all $\omega \leq \omega_A$ and $\omega \geq \omega_B$ the effect is to move the new L away from the boundaries, thus creating pockets of "surplus" which may be exploited by the techniques of Conditions 1-3 . In part of the range $\omega_A \leq \omega \leq$ B , the effect of F_c is to push L towards the boundaries but a surplus exists in this range for this purpose.

From the above four conditions, for boundaries of negative slope, it follows that the optimum L , if it exists, must lie at each frequency, on its boundary. The next step is to prove that such an L , if it exists, is unique, if its value is fixed at $\omega = 0$.

3.3 Uniqueness of L with prescribed L(0)

Theorem.

There cannot be two or more $L(j\omega)$ functions, which lie on the boundaries for all $\omega > 0$ and which are equal at $\omega = 0$. (Proven only for boundaries of negative slope.)

Proof.

Suppose that it is not so and there are two of them, L_A and L_B , with $L_A(0) = L_B(0)$. There are three possibilities, as shown in Fig. 3.9 . L_{B1} is for the case $|L_B| \geq |L_A|$ for all ω , in which case $\theta_B \leq \theta_A$ for all ω . L_{B2} is for the case $|L_B| \leq L_A$ for all ω , in which case $\theta_B \geq \theta_A$ for all ω . L_{B3} is for the last possible case when L_B crosses L_A at one or more points. (Note that at $\omega = 0$, in a type zero system, $L(0)$ must lie on the vertical line $\theta = 0$. In a type 1 system there is a lower bound on lim, $sL(s)$, and $sL(0)$ must lie on the vertical line $\theta \overset{s \to 0}{\geq} -90°$.) Consider

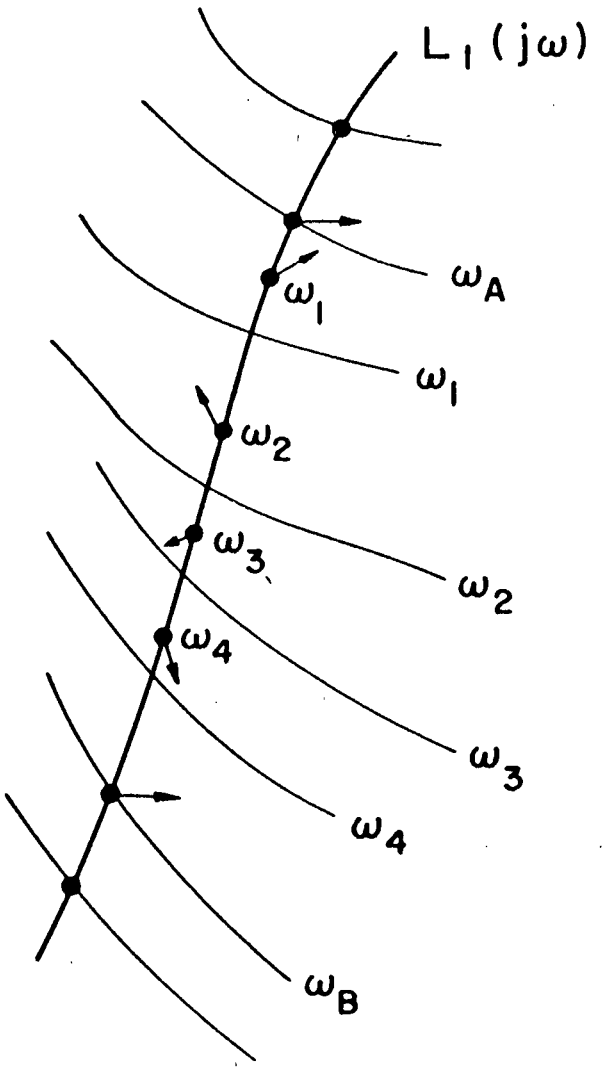

Fig. 3.8: Proof of necessary condition 4

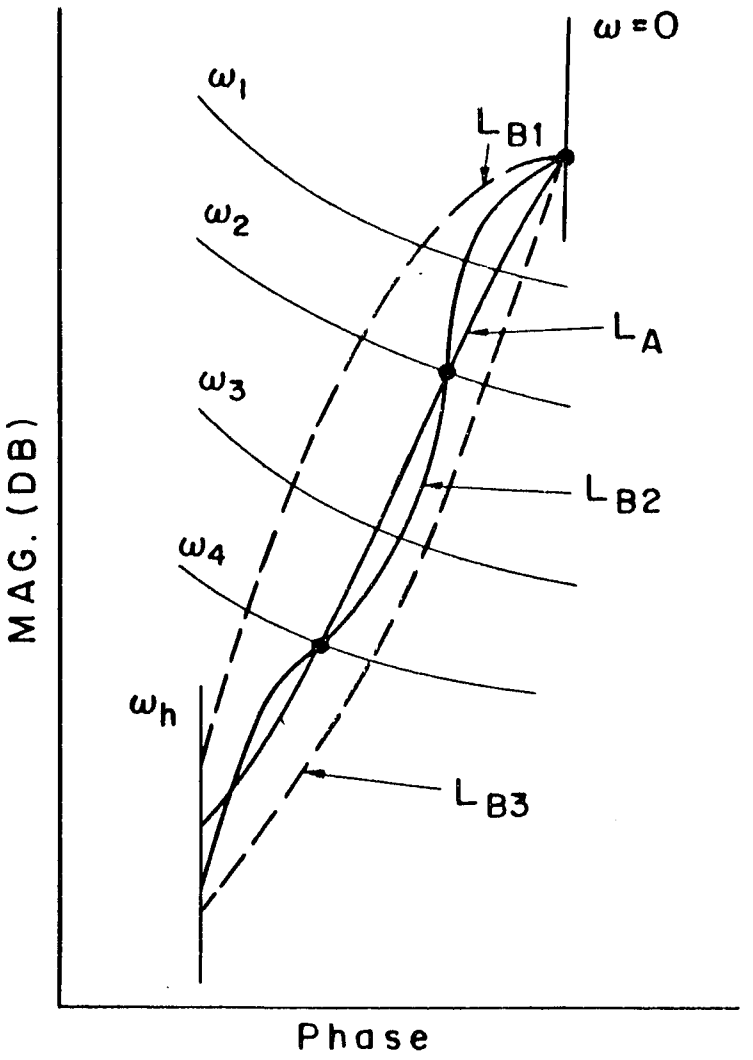

Fig. 3.9: The three L_B possibilities

$L_i \triangleq L_A/L_{Bi}$ for the three L_B cases. Magnitude and phase sketches of $|L_i|_{DB}$ and θ_i are shown in Fig. 3.10, for the three.

Apply the relation[16] (which applies to minimum-phase L_i)

$$\frac{4}{\pi}\int_{\infty}^{\infty}\theta_i \ell n|L_i|\frac{d\omega}{\omega} = (\ell n|L_i(j\infty|))^2 - (\ell n|L_i(0)|)^2 \qquad (3.5)$$

to each L_i. Since $L_i(0) = 1$, the righthand side of (3.5) is positive. However, from Fig. 3.10, it is seen that whenever $\theta_i \geq 0$, $\ell n|L_i| \leq 0$ and vice versa. Hence the left-hand side of Equation (3.5) must be negative. Thus the supposition is untenable and there can be only one such loop transfer function. It is very important to note that this proof depends on boundaries with negative slope as in Fig. 3.9, for only then is $\theta_B < \theta_A$ when $|L_B| > |L_A|$.

The above theorem does not preclude an infinitude of $L_I(j\omega)$, providing each has a different value at zero frequency.

3.4 Optimum L has minimum permissible value at $\omega = 0$

The next step is to prove that the best L is the one with minimum magnitude at $\omega = 0$ (or for Type 1 systems the one with minimum value of $\lim_{s\to 0} sL(s)$, etc). This is done by means of the following relation, for minimum-phase F(s),

$$\int_0^{\omega_c} \frac{[\ell n|F(j\omega)| - \ell n|F(\infty)|]d\omega}{\sqrt{1 - \frac{\omega^2}{\omega_c^2}}} = -\int_{\omega_c}^{\infty} \frac{\theta d\omega}{\sqrt{\frac{\omega^2}{\omega_c^2} - 1}} \qquad (3.6)$$

where

$$F = |F| \angle\theta \quad . \qquad (3.7)$$

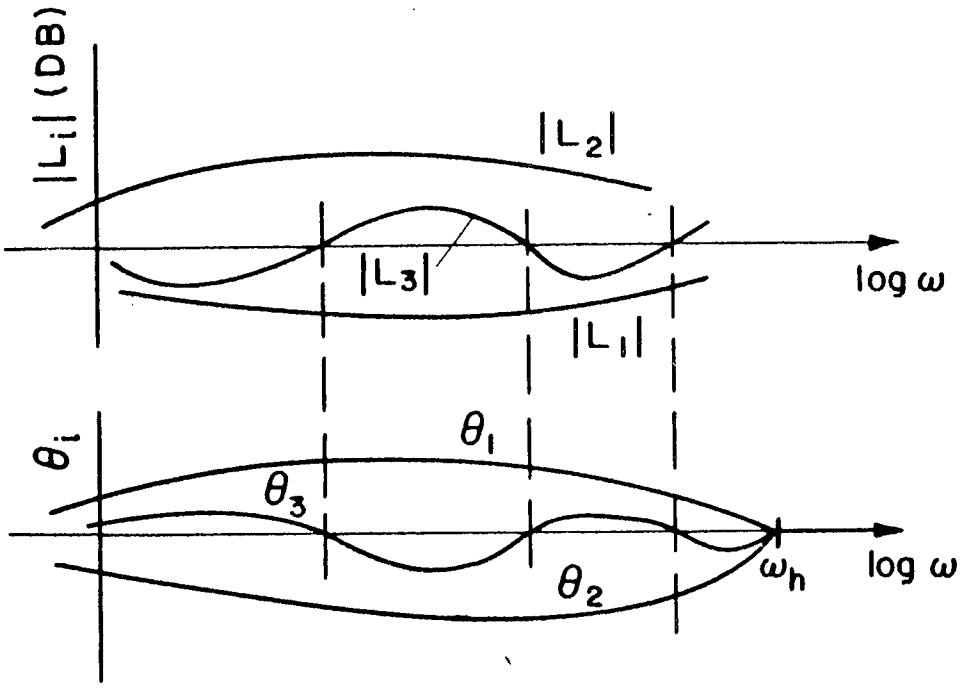

Fig. 3.10: Proof of uniqueness

Theorem. The optimum L must have the minimum permissible magnitude at $\omega = 0$.

Proof.

Consider $L_m(s)$ with (1) the minimum permissible magnitude at $\omega = 0$ and (2) which crosses the boundaries at each value of ω. Compare it to any other $L_1(s)$ which satisfies (2) but is larger than L_m at $\omega = 0$. $L_m(j\omega)$ can cross $L_1(j\omega)$ either an even or an odd number of times in the range $0 \leq \omega \leq \omega_h$. If they do not cross at all in this range, then the situation can be as shown in Fig. 3.11, for $F \triangleq L_1/L_m$. Case (a) or any even number of crossings in the range $\omega > \omega_h$ leads to

$$|F|_\infty = |L_1/L_m(\infty)| \geq 1 \quad , \tag{3.8}$$

so there is no advantage in L_1 over L_2. Case (b), applied to Equation (3.6) with $\omega_c = \omega_h$, has zero for the right-hand side. On the left side $\ell n|F(\infty)| \leq 0$. Hence the integrand is always positive. This is a contradiction in that the left side is finite and positive, the right side zero. Hence case (b) is impossible. We next turn to the case of even number of crossings in the range $0 < \omega < \omega_h$.

Case 1 Even number of crossings in the range $0 < \omega < \omega_h$

In this case $F(j\omega) \triangleq L_1(j\omega)/L_m(j\omega)$ will appear qualitatively as in Fig. 3.12. Sub-case (i) or of any even number of crossings in the range $\omega > \omega_h$ need not be considered, for then (3.8) applies. Only sub-case (ii), i.e., an odd number of crossings in the range $\omega > \omega_h$ need be considered.

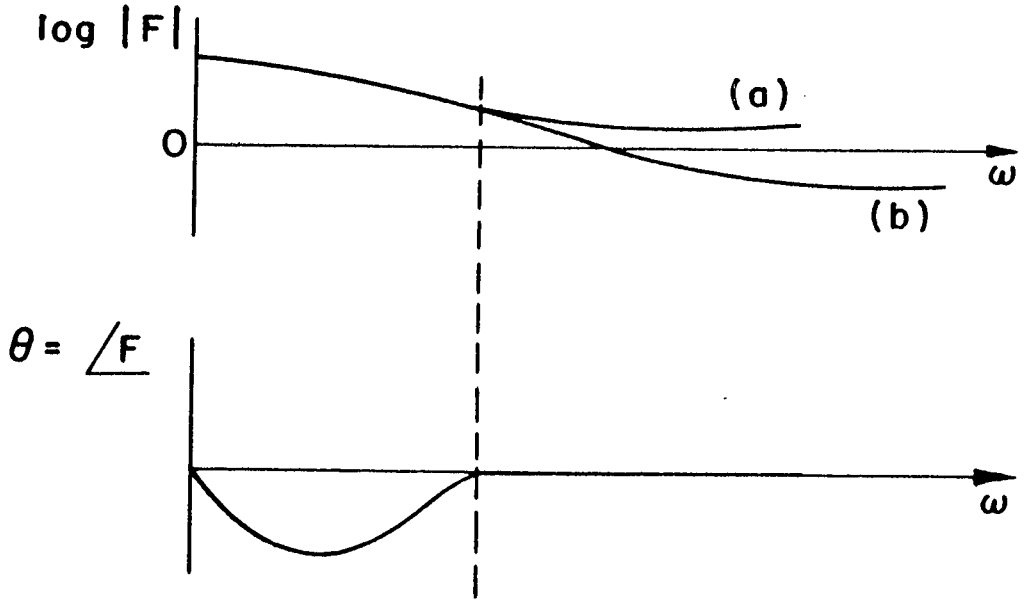

Fig. 3.11: Options when L's do not cross

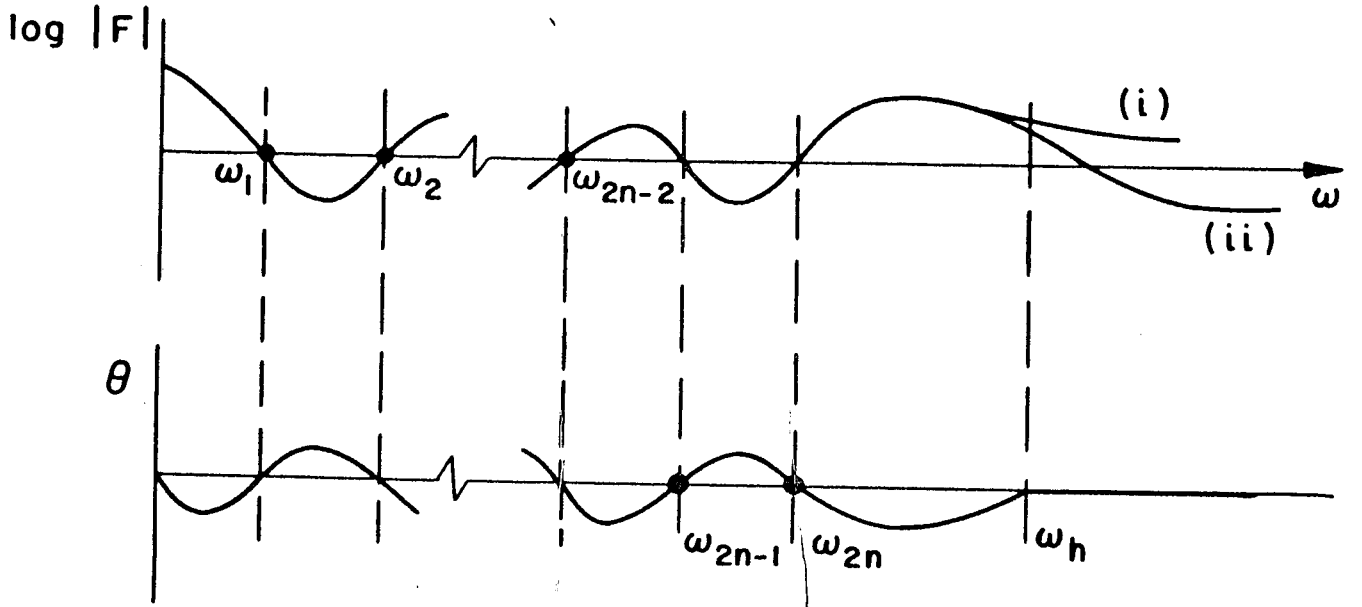

Fig. 3.12: Even number of crossings

Let $\omega_h = \omega_c$ of Equation (3.6) and write $\ell n|F(\infty)| = -M$, $M > 0$ because, for subcase (ii), $|F(\infty)| < 1$. Equation (3.6) can be written as follows

$$(\alpha_1-\alpha_2) + (\alpha_3-\alpha_4) + \cdots + (\alpha_{2n-1}-\alpha_{2n}) + \mu_1 + \mu_2 = 0 \qquad (3.9)$$

where

$$\alpha_{2i+1} = \int_{\omega_{2i}}^{\omega_{2i+1}} \frac{\ell n|F|\,d\omega}{\sqrt{1 - \frac{\omega^2}{\omega_h^2}}} \qquad (3.10a)$$

$$\alpha_{2i} = \left|\int_{\omega_{2i-1}}^{\omega_{2i}} \frac{\ell n|F|\,d\omega}{\sqrt{1 - \frac{\omega^2}{\omega_h^2}}}\right| \qquad (3.10b)$$

$$\mu_1 = \int_{\omega_{2n}}^{\omega_h} \frac{\ell n|F|\,d\omega}{\sqrt{1 - \frac{\omega^2}{\omega_h^2}}} \qquad (3.11a)$$

$$\mu_2 = M \int_0^{\omega_h} \frac{d\omega}{\sqrt{1 - \frac{\omega^2}{\omega_h^2}}} = \frac{\pi}{2} M \omega_h > 0 \,. \qquad (3.11b)$$

Next, let $\omega_{2n} = \omega_c$ of Equation (3.6), which becomes

$$(\beta_1-\beta_2) + (\beta_3-\beta_4) + \cdots + (\beta_{2n-1}-\beta_{2n}) + \mu_2 - \varepsilon > 0 \qquad (3.12)$$

because on the right-hand side of (3.6), $\theta < 0$ in the range $\omega_c = \omega_{2n} < \omega < \omega_h$. In (3.12),

$$\beta_{2i+1} = \int_{\omega_{2i}}^{\omega_{2i+1}} \frac{\ell n|F|d\omega}{\sqrt{1 - \frac{\omega^2}{\omega_{2n}^2}}} \tag{3.13a}$$

$$\beta_{2i} = |\int_{\omega_{2i-1}}^{\omega_{2i}} \frac{\ell n|F|d\omega}{\sqrt{1 - \frac{\omega^2}{\omega_{2n}^2}}} \tag{3.13b}$$

The last two terms on the left-hand side of (3.12) constitute

$$-\int_0^{\omega_{2n}} \frac{\ell n|F(\infty)|d\omega}{\sqrt{1 - \frac{\omega^2}{\omega_{2n}^2}}} = \frac{\pi}{2}M\omega_{2n} < \frac{\pi}{2}M\omega_{2h} , \tag{3.13c}$$

which can be written as $\frac{\pi}{2}M\omega_{2h} - \varepsilon = \mu_2 - \varepsilon$ with $\varepsilon > 0$.

Compare any pair $(\alpha_{2i-1} - \alpha_{2i+2})$ of Equation (3.9) with $(\beta_{2i+1} - \beta_{2i+2})$ of Equation (3.12) .

$$\alpha_{2i+1} - \alpha_{2i+2} = \int_{\omega_{2i}}^{\omega_{2i+1}} \left[\frac{1 - \frac{\omega^2}{\omega_{2n}^2}}{1 - \frac{\omega^2}{\omega_h^2}}\right]^{0.5} \frac{\ell n|F|d\omega}{\sqrt{1 - \frac{\omega^2}{\omega_{2n}^2}}}$$

$$-|\int_{\omega_{2i+1}}^{\omega_{2i+2}} \left[\frac{1 - \frac{\omega^2}{\omega_{2n}^2}}{1 - \frac{\omega^2}{\omega_h^2}}\right]^{0.5} \frac{\ell n|F|d\omega}{\sqrt{1 - \frac{\omega^2}{\omega_{2n}^2}}} . \tag{3.14a}$$

The function $\rho(\omega) \triangleq \left[\dfrac{1 - \dfrac{\omega^2}{\omega_{2n}^2}}{1 - \dfrac{\omega^2}{\omega_h^2}}\right]^{0.5}$ (3.14b)

is monotonically decreasing for $0 \leq \omega \leq \omega_{2n}$. Hence, $\rho(\omega_{2i+1}) < \rho(\omega)$ for the open interval of integration of the first term on the right side of (3.14a) , while $\rho(\omega_{2i+1}) > \rho(\omega)$ for the open interval of integration of the second term. But note that if $\rho(\omega)$ is removed from these integrals, what remains are precisely the integrands of β_{2i+1} , β_{2i+2} , respectively, and over the same limits of integration. Hence

$$\alpha_{2i+1} > \rho(\omega_{2i+1})\beta_{2i+1} \; ; \quad \alpha_{2i+2} < \rho(\omega_{2i+1})\beta_{2i+2} \tag{3.15}$$

$$\alpha_{2i+1} - \alpha_{2i+2} > \rho(\omega_{2i+1})(\beta_{2i+1} - \beta_{2i+2}) \tag{3.16}$$

Note also, because of the monotonically decreasing nature of $\rho(\omega)$, that

$$1 > \rho_1 > \rho_2 \cdots > \rho_{2n-1} > 0 \; . \tag{3.17}$$

Combining (3.16) and (3.17), gives

$$\begin{aligned}
&(\alpha_1 - \alpha_2) + (\alpha_3 - \alpha_4) + \cdots (\alpha_{2n-1} - \alpha_{2n}) \\
&> \rho(\omega_1)(\beta_1 - \beta_2) + \rho(\omega_3)(\beta_3 - \beta_4) + \cdots \rho(\omega_{2n-1})(\beta_{2n-1} - \beta_{2n}) \\
&> \rho(\omega_{2n-1})[(\beta_1 - \beta_2) + (\beta_3 - \beta_4) + \cdots (\beta_{2n-1} - \beta_{2n})] \\
&> \rho(\omega_{2n-1})(-\mu_2 + \varepsilon) \; ,
\end{aligned} \tag{3.18}$$

from (3.12) .

But, from (3.9), the left side of (3.18), i.e.,
$(\alpha_1-\alpha_2) + \cdots = -(\mu_1+\mu_2)$.

Hence,

$$-(\mu_1+\mu_2) > \rho(\omega_{2n-1})(-\mu_2+\varepsilon) \tag{3.19}$$

or

$$-\mu_1-\varepsilon\rho(\omega_{2n-1}) > \mu_2[1-\rho(\omega_{2n-1})] > 0 \ . \tag{3.20}$$

because $0 < \rho(\omega_{2n-1}) < 1$.

Since μ_1 , ε , ρ are all positive (3.20) is impossible, so the hypothesis is untenable.

Case 2. Odd number of crossings

In this case $F(j\omega) \triangleq L_1(j\omega)/L_2(j\omega)$ will appear qualitatively as in Fig. 3.13. Sub-case (i) in Fig. 3.13, or of any even number of crossings in the range $\omega > \omega_h$, need not be considered, for then (3.8) applies. Only sub-case (ii), i.e., an odd number of crossings in the range $\omega > \omega_h$, needs to be shown impossible.

Let ω_c of Equation (3.6) be set equal to ω_{2n+1} . Then Equation (3.6) becomes

$$(\alpha_1-\alpha_2) + (\alpha_3-\alpha_4) + \cdots + (\alpha_{2n-1}-\alpha_{2n}) + \alpha_{2n+1}$$

$$+ \frac{\pi M}{2}\omega_{2n+1} = -\int_{\omega_{2n+1}}^{\omega_h} \frac{\theta d\omega}{\sqrt{\frac{\omega^2}{\omega_{2n+1}^2} - 1}} \triangleq -\alpha < 0 \tag{3.21}$$

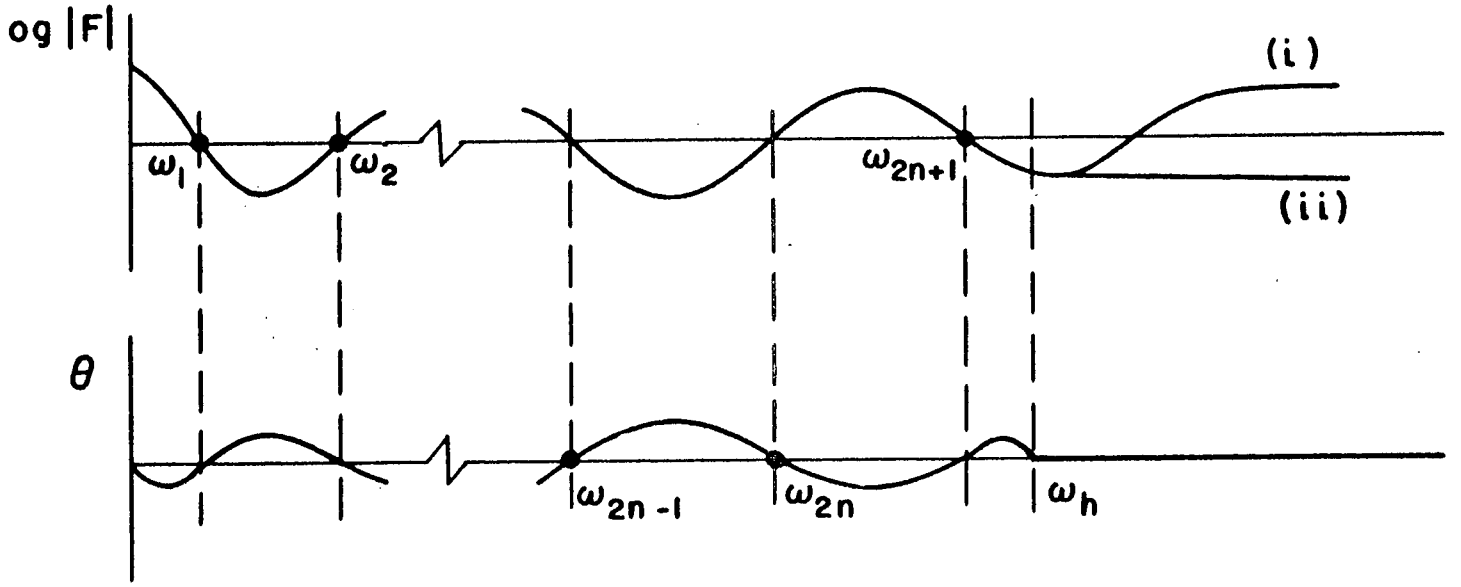

Fig. 3.13: Odd number of crossings

where the α_i are defined as before, in Equations (3.10a,b), except for the substitution of ω_{2n+1} for ω_h .

Let $\omega_c = \omega_{2n}$ in Equation (3.6), and it becomes

$$(\beta_1-\beta_2)+(\beta_3-\beta_4)+\cdots+(\beta_{2n-1}-\beta_{2n})+\frac{\pi M}{2}\,\omega_{2n} = \int_{\omega_{2n}}^{\omega_h} \frac{\theta d\omega}{\frac{\omega^2}{\omega_{2n}^2}-1} = -\alpha+\beta, \quad (3.22)$$

with $\beta > 0$, since

$$\alpha = \int_{\omega_{2n+1}}^{\omega_h} \frac{\theta d\omega}{\frac{\omega^2}{\omega_{2n+1}^2}-1} > \int_{\omega_{2n}}^{\omega_h} \frac{\theta d\omega}{\frac{\omega^2}{\omega_{2n}^2}-1} ,$$

because $\omega_{2n+1} > \omega_{2n}$ and because $\theta < 0$ in the range $\omega_{2n} < \omega < \omega_{2n+1}$.

As in the previous development,

$$(\alpha_{2i+1}-\alpha_{2i+2}) > \lambda(\omega_{2i+1})(\beta_{2i+1}-\beta_{2i+2}) \quad (3.23a)$$

with

$$\lambda(\omega) = \left[\frac{1-\frac{\omega^2}{\omega_{2n}^2}}{1-\frac{\omega^2}{\omega_{2n+1}^2}}\right]^{0.5} , \quad (3.23b)$$

monotonically decreasing from unity over the range $0 < \omega < \omega_{2n}$, i.e.,

$$1 > \lambda(\omega_1) > \lambda(\omega_2) \cdots\cdots > \lambda(\omega_{2n-1}) > 0 .$$

Therefore

$$(\alpha_1-\alpha_2)+\cdots+(\alpha_{2n-1}-\alpha_{2n})>\rho(\omega_{2n-1})[(\beta_1-\beta_2)+\cdots+(\beta_{2n-1}-\beta_{2n})] \quad . \quad (3.24)$$

From Equations (3.21, 3.22), this means

$$-\alpha-\frac{\pi M\omega_{2n+1}}{2}-\alpha_{2n+1} > \rho(\omega_{2n-1})[-\alpha+\beta-\frac{\pi M\omega_{2n}}{2}] \quad (3.25)$$

which can be manipulated into

$$(\alpha+\frac{\pi M\omega_{2n}}{2})[1-\rho(\omega_{2n-1})]+\frac{\pi M}{2}(\omega_{2n+1}-\omega_{2n})<-\alpha_{2n+1}-\beta\rho(\omega_{2n-1}) \quad . \quad (3.26)$$

Each factor of each term on the left is positive, while each term on the right is negative. Therefore the assumption (ii) of Fig. (3.12) is impossible.

So far, it has been found that the optimum L, if it exists, must lie at each frequency on a boundary curve and have the minimum permissible value at $\omega = 0$. It has also been proven that such an L, if it exists, is also unique. There therefore only remains to prove that such an $L(s)$ does indeed exist.

Existence Theorem

There exists an optimum L function in the sense previously described.

Proof

We use the analogue of the Weierstrass Theorem which states[18] that if $J(f)$ is a continuous functional defined on the normal and compact family $\{f(z)\}$, then $|J(f)| = \text{MIN}$

has a solution within this family. In this problem $J(f) = J[L(j\omega)] = \lim_{\omega \to \infty} |(j\omega)^x L(j\omega)|$, where x is chosen so that J is nonzero and finite; for example, if the vertical boundary for $\omega \geq \omega_h$ is at $-\theta$, then $x = 2\theta/\pi$. Such a functional is clearly continuous for a large variety of norms. There is a theorem [19] which states that a class of analytic functions regular and uniformly bounded in a domain D is a normal family which is also compact. Uniformly bounded functions $f(s)$ in D are those for which there exists a positive constant M, such that $|L(s)| \leq M$, for s in D. In this case D is the right half-plane and $L(s)$ is regular in D. For any given problem it is always possible to select an M such that the family of candidate L functions is restricted to $|L(j\omega)| < M$ for all ω. [For a Type 1 system, one would deal with $sL(s)$, etc.] By the principle of the maximum modulus, $|L(s)| < M$ in D. Hence, all the conditions of the theorem are satisfied and our functional must have a minimum.

CHAPTER IV

PROPERTIES OF OPTIMUM $L(j\omega)$ - NECESSARY CONDITIONS FOR BOUNDARIES OF BOTH POSITIVE AND NEGATIVE SLOPE

4.1 Introduction

This chapter is devoted to the derivation of some properties of the optimum $L(j\omega)$ function, for the case when the boundary curves can have portions with positive slope, as for example in Fig. 4.1. In contrast with Chapter 3, a complete theory has not been developed. An important necessary condition has been found, and exactly the same existence theorem as in Chapter 3 applies to this case. However, sufficiency, proven implicitly in Chapter 3 by proving uniqueness, has not been proven here for the function which satisfies the necessary condition.

4.2 Some necessary conditions for the optimum $L(s)$

The first two conditions were proven in Chapter 3, as necessary conditions 1,2 .

(1) For all $\omega \geq \omega_h$, the optimum $L(j\omega)$ must lie on the vertical line V (Fig. 4.1).

(2) The optimum L must lie on the boundaries in the frequency range immediately below ω_h .

(3) The optimum L must be on the boundaries in the region where the boundaries have negative slope.

The third necessary condition is restricted to the case where $L(j\omega)$ passes initially through a region of positive slope boundaries, followed by a region of negative slope boundaries.

Proof

The building block F_1 of Fig. 4.2 is used in the proof. Suppose the postulated L lies above some positive slope boundaries, as shown in Fig. 4.1 . Then $L_2 = F_1 L$ will have the values in the direction of the arrows, and will have a

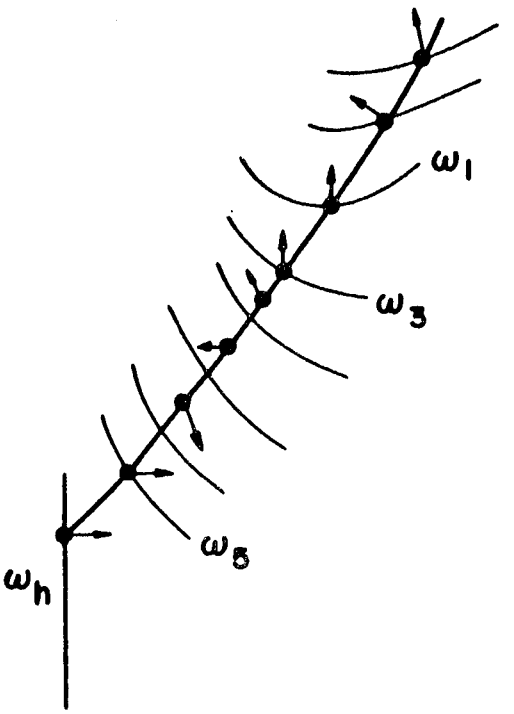

Fig. 4.1: Proof of necessary condition 3

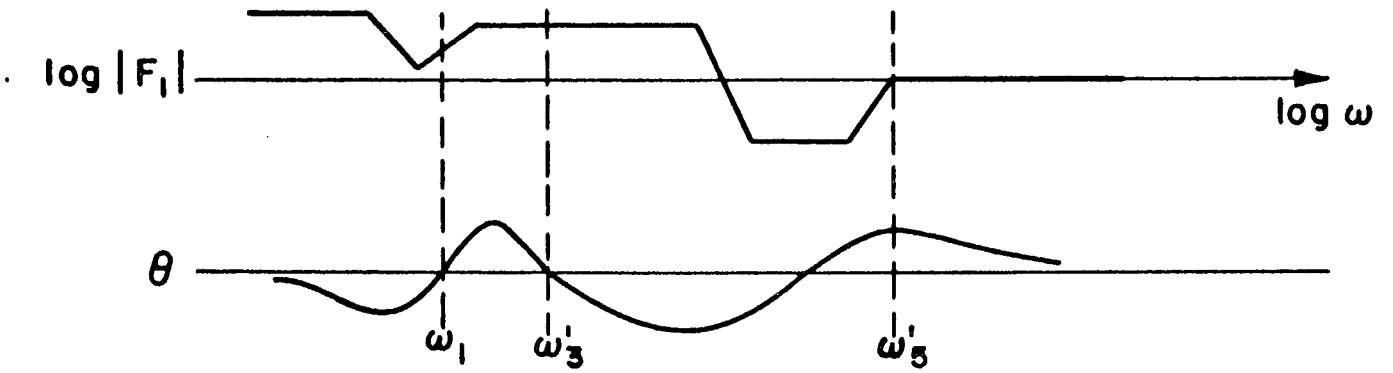

Fig. 4.2: Building block F_1 for necessary condition 3

finite'surplus' for all $\omega > \omega_5'$. The technique of necessary conditions 1,2 can be used to exploit this surplus. Note that for the proof to be valid it is necessary that $\omega_1' = \omega_1$, and that the range (ω_3', ω_5') of the building block of Fig. 4.2 be chosen so that it lies inside the range (ω_3, ω_5) of Fig. 4.1 . This is evidently always possible to do with the many parameters available, i.e., the various levels and slopes of F_1 .

Generalization. More complex building blocks are required, in order to generalize this result to the case when $L(j\omega)$ passes through several alternating regions of positive and negative slopes. For example, that in Fig. 4.3 may be used for the following order of slopes (starting from $\omega = 0$): positive, negative, positive, negative, and with a surplus pocket in the last negative region, as shown in Fig. 4.4 . Obvious extensions of Fig. 4.3 would apply for larger number of pairs of alternating slopes with the last being negative, and wherein a surplus pocket exists in the last region.

4.3 Necessary condition 4

This condition applies to the case where $L(j\omega)$ passes initially through a region of positive slope, followed by a region of negative slope boundaries.

(4) The optimum L must lie on the boundaries in the region of positive slope.

Building Block

A somewhat more elaborate building block is needed for the proof of (4) . It is constructed from Fig. 4.5, where $|L|$ is specified to be zero db from $\omega = 0$ to $\omega = \omega_A$, while $\theta = \angle L$ is specified with the indicated properties for

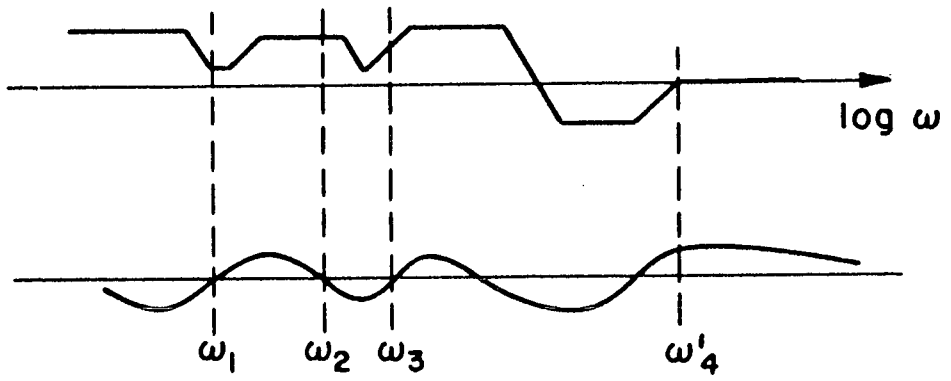

Fig. 4.3: Building block for extension of necessary condition 3

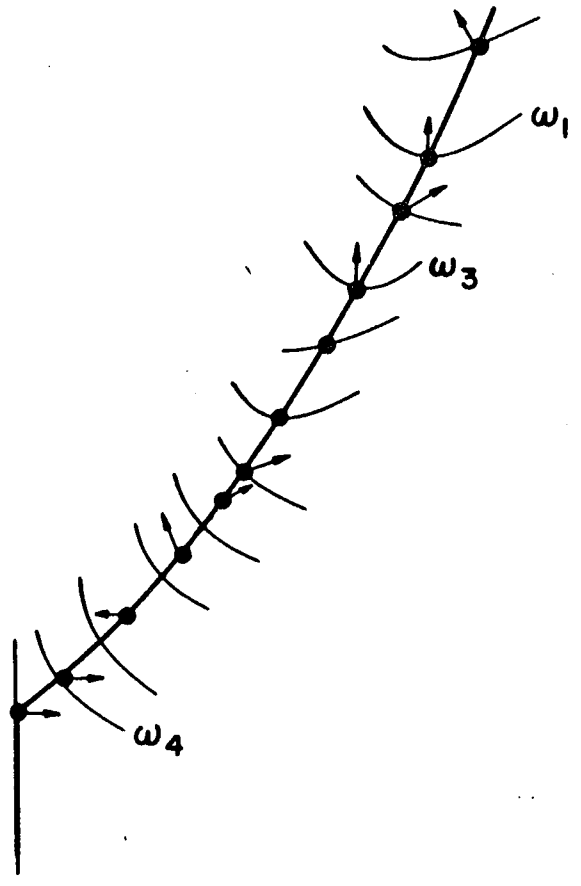

Fig. 4.4: Extension of necessary condition 3

$\omega_A < \omega$; i.e., $\theta < 0$ for $\omega_A < \omega < \omega_x$, $\theta > 0$ for $\omega_x < \omega < \omega_B$, $\theta = 0$ for $\omega > \omega_B$. Also θ is continuous so $\theta = 0$ at $\omega = \omega_A, \omega_x, \omega_B$. The missing portions ($|L|$ for $\omega > \omega_A$, and θ for $\omega < \omega_A$), may be obtained from the appropriate Bode integrals[20,21], which here simplify into

$$\int_{\omega_A}^{\omega_B} \frac{\theta d\xi}{(\omega^2-\xi^2)(\xi^2-\omega_A^2)^{0.5}} = \frac{-\pi\theta(\omega)}{2\omega(\omega_A^2-\omega^2)^{0.5}} \quad \text{for} \quad \omega < \omega_A \tag{4.1a}$$

$$= \frac{|M(\omega)|}{2\omega(\omega^2-\omega_A^2)^{0.5}} \quad \text{for} \quad \omega > \omega_A \tag{4.1b}$$

where

$$M(\omega) \triangleq \ell n|L(j\omega)| \tag{4.2}$$

It will be shown that it is possible to choose θ of the form indicated in Fig. 4.5, in the range $\omega_A < \omega < \omega_B$, such that the complete L is as shown in Fig. 4.6. The important features are: the range of positive M for $\omega > \omega_y > \omega_x$, the ability for $\log|F|$ to be zero at infinity, or alternatively to cross at $\omega_z > \omega_B$ from positive to negative values; and to remain negative from ω_z to infinity.

The proof of the above assertions will be given by selecting a specific form for $\theta(\omega)$, with sufficient parameters to obtain these properties at prespecified frequencies.

Selection of $\theta(\omega)$ in range $\omega_A \leq \omega \leq \omega_B$

Let $\theta(\xi) = \sqrt{\xi^2-\omega_A^2}\,(A + B\xi + C\xi^2)$, for $\omega_A \leq \omega \leq \omega_B$, (4.3)

with $\theta(\omega_A) = \theta(\omega_x) = \theta(\omega_B) = 0$. (4.4)

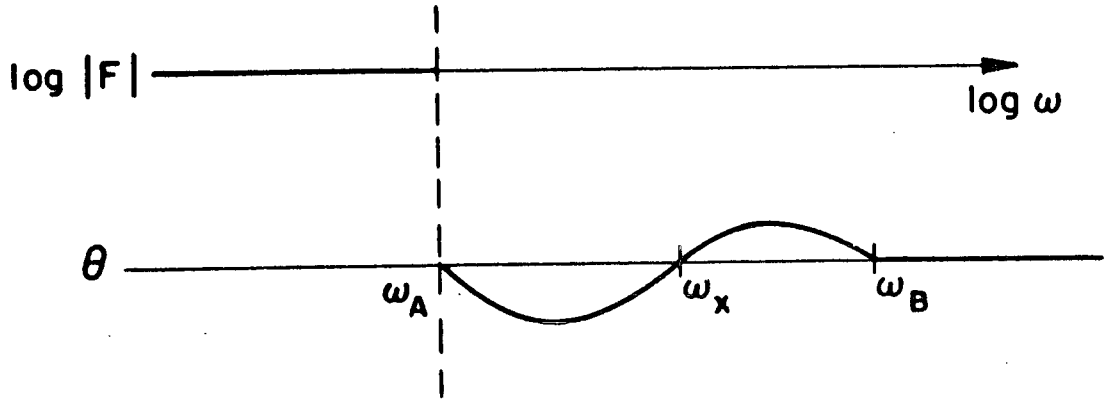

Fig. 4.5: Log |F| defined for $\omega < \omega_A$; θ defined for $\omega > \omega_A$

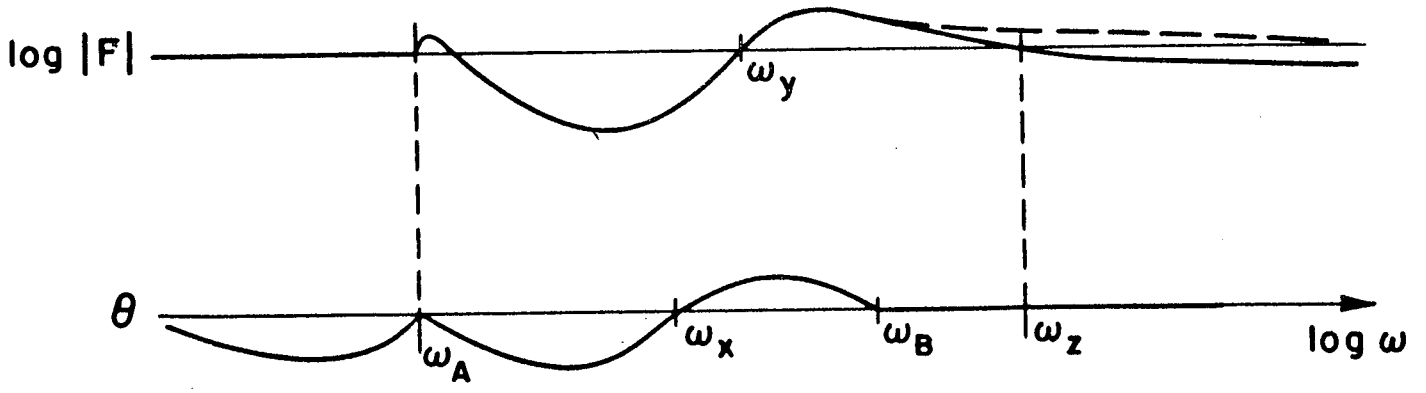

Fig. 4.6: Completed F

Hence

$$0 = A + B\omega_x + C\omega_x^2 \; ; \; 0 = A + B\omega_B + C\omega_B^2 \qquad (4.5a,b)$$

Solution of (4.5a,b) gives

$$B = - A \frac{(\omega_x+\omega_B)}{\omega_x\omega_B} \; ; \quad C = \frac{A}{\omega_x\omega_B} \qquad (4.6a,b)$$

so that only A and ω_x remain to be chosen. Consider the sign of $M(\infty)$ which we would like to be negative or zero. From (4.1b, 4.3, 4.6a,b), this requirement is

$$A \int_{\omega_A}^{\omega_B} [1 - \frac{(\omega_x+\omega_B)\xi}{\omega_x\omega_B} + \frac{\xi^2}{\omega_x\omega_B}] d\xi \leq 0 \; . \qquad (4.7)$$

It is easy to see that $A < 0$ in order that $\theta(\omega_B^-) > 0$, because

$$\theta(\omega_B^-) = \frac{A[\omega_x\omega_B - (\omega_x+\omega_B)\omega_B^- + (\omega_B^-)^2]}{\omega_x\omega_B} = \frac{A(\omega_x-\omega_B^-)(\omega_B-\omega_B^-)}{\omega_x\omega_B} \; .$$

With $A < 0$, (4.7) gives

$$\omega_B'(3\omega_x'-\omega_B') - (\omega_B'+3\omega_x') + 2 \geq 0 \qquad (4.8)$$

where the primes indicate normalization with respect to ω_A, i.e., $\omega_B' = \omega_B/\omega_A$ etc.

If $3\omega_x' = \omega_B'$, then (4.8) requires $2 \geq \omega_B' + 3\omega_x'$, which is impossible. A necessary condition for (4.8) is therefore

$$\frac{3\omega_x'}{\omega_B'} > 1 \qquad (4.9a)$$

and condition (4.8) can be written as

$$\frac{\omega_x}{\omega_B} = \rho = \frac{\omega_x'}{\omega_B'} \geq \frac{\omega_B'+2}{3\omega_B'} \quad . \tag{4.9b}$$

For example, if $\omega_B' = 2$, then $\rho = 2/3$ gives $M(\infty) = 0$, while $\rho > 2/3$ gives $M(\infty) < 0$. Also obviously, ρ can be chosen to precisely position ω_z (of Fig. 4.6).

For our purposes it is important that $M(\omega_B^-) > 0$. Evaluating (4.1b) with $\theta(\xi)$ of Equation (4.3), gives

$$M = \psi \sqrt{1 - \frac{\omega_A^2}{\omega^2}} \quad \text{for} \quad \omega > \omega_A \ , \tag{4.10a}$$

$$\theta = -\psi \sqrt{\frac{\omega_A^2}{\omega^2} - 1} \quad \text{for} \quad \omega < \omega_A \ . \tag{4.10b}$$

$$\psi = A \frac{\omega^2}{\pi} \left[B_1 \ell n \left| \frac{\omega_B - \omega}{\omega_A - \omega} \right| + B_2 \ell n \left| \frac{\omega_B + \omega}{\omega_A + \omega} \right| - 2 \left(\frac{\omega_B - \omega_A}{\omega_x \omega_B} \right) \right] \tag{4.10c}$$

$$\omega_x \omega_B B_1 = \omega_x + \omega_B - \left(\omega + \frac{\omega_x \omega_B}{\omega} \right) \tag{4.10d}$$

$$\omega_x \omega_B B_2 = \omega_x + \omega_B + \left(\omega + \frac{\omega_x \omega_B}{\omega} \right) \ . \tag{4.10e}$$

From the above it is found that $M(\omega_B^-) > 0$ requires

$$\rho = \frac{\omega_x}{\omega_B} < \frac{1 - \frac{1}{\omega_B'}}{\ell n \frac{2\omega_B'}{1+\omega_B'}} - 1 \ . \tag{4.11}$$

Combining (4.9b), (4.11) gives

$$\frac{\omega_B'^2 + \omega_B' - 2}{3\omega_B(\omega_B - 1)} < \frac{1 - \frac{1}{\omega_B'}}{\ell n \frac{2\omega_B'}{1+\omega_B'}} - 1 \tag{4.12a}$$

which reduces to

$$\ell n \ \frac{2}{\alpha+1} < \frac{1.5(1-\alpha)}{(2+\alpha)} \tag{4.12b}$$

where

$$\alpha = \frac{1}{\omega_B'} = \frac{\omega_A}{\omega_B} \ . \tag{4.12c}$$

It is easily found that (4.12b) applies for $0 < \alpha < 1$.

If Equations (4.10) are expanded at $\omega = \omega_A + \delta$, the result is $M \to KA \sqrt{\delta}\, \ell n\, \delta$, with $K > 0$. Since $A < 0$, $M > 0$ at $\omega = \omega_A + \delta$. Similarly, it is found that $\theta < 0$ at $\omega = \omega_A - \delta$. At $\omega = \delta$, θ is negative, if

$$(1+ \frac{1}{\rho}) > \frac{\beta-1}{\ell n \beta} \tag{4.13}$$

where $\rho = \frac{\omega_x}{\omega_B} < 1$, $\beta = \frac{\omega_B}{\omega_A}$, which is always satisfied, as $\beta > 1$. It is known that both M and θ of Fig. 4.6 are continuous and the shape of the characteristics for frequencies in between the above calculated points, as shown in Fig. 4.6, has been checked by numerous computer runs.

Application of Building Block to prove Necessary Condition 4

In Fig. 4.7 there is sketched a set of boundaries and an L function with the properties under consideration. Let $L_2 = FL$ with F like that in Fig. 4.6. Choose $\omega_A \geq \omega_A'$, $\omega_B \leq \omega_B'$, and $\omega_h \leq \omega_z$. The values of L_2 are in the direction of the arrows in Fig. 4.7 (for the case these relations are satisfied with the equality sign). Hence, clearly L_2 is better than L .

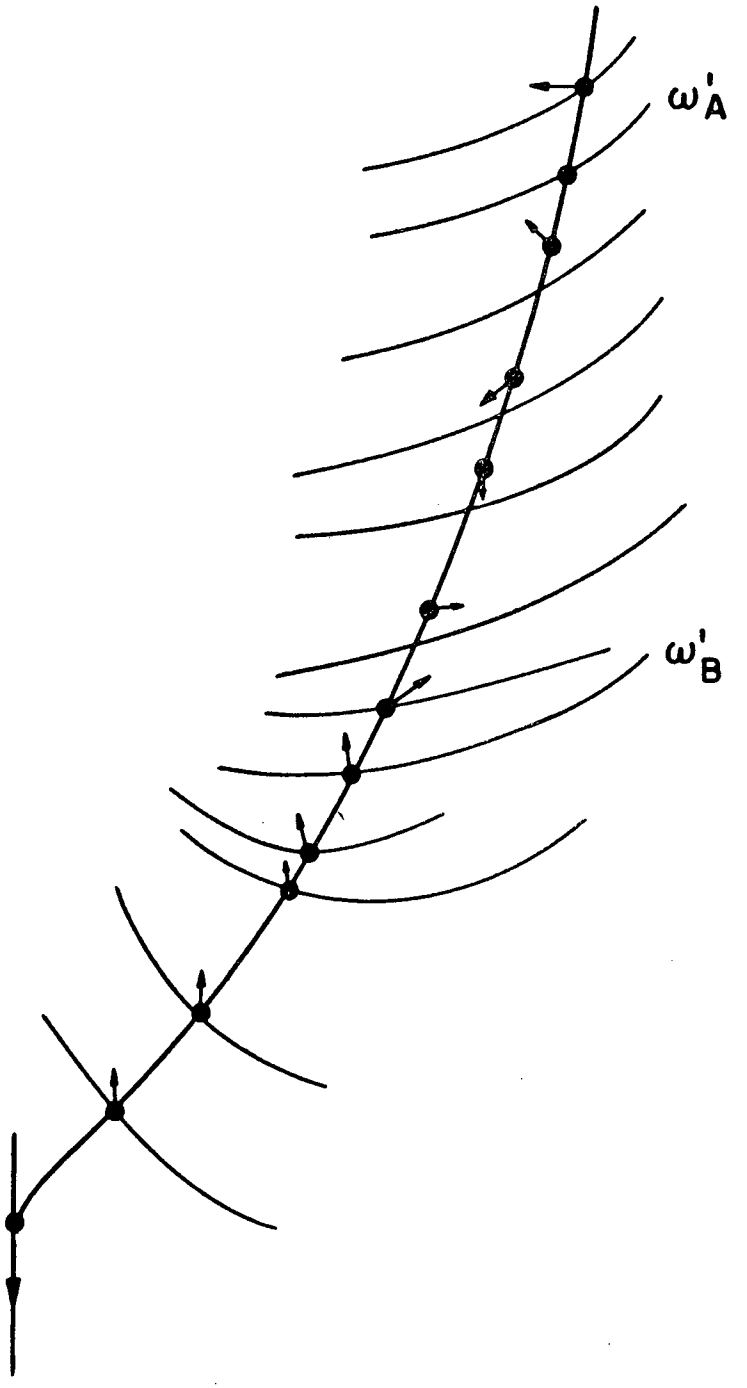

Fig. 4.7: Necessary condition 4

Generalization

Consider the sequence of frequency ranges with a trial L crossing in order, boundaries of positive, negative, positive, negative slopes, with a surplus in the last positive range. Part of the building block of Fig. 4.2, properly combined with that of Fig. 4.6, could presumably be used for a building block. But this has not been explored.

Summary

It has been shown that a necessary condition for an optimum L which passes through a range of positive boundary slopes, followed by one of negative slopes, is that L must lie on the boundaries at every frequency. The existence theorem of Chapter 3 is also valid and indicates that an optimum L does exist, but, of course, it need not cross the boundaries in the above manner. It may be such as to cross only negative slope boundaries or to cross alternately more than two different sign slopes. Intuition and experience suggest that for all cases the optimum must lie on the boundaries.

CHAPTER 5

SHAPING OF THE LOOP TRANSMISSION FUNCTION

5.1 Introduction

It is assumed that the boundaries of L for a suitable number of discrete frequencies have been obtained, as in Chapter 2. From the work in Chapter 3, 4 it is concluded that the optimum L is one which lies on the respective boundaries at each frequency. The objective is to achieve such an $L(s)$ function. Some guide lines are presented here for this purpose.

5.2 Detailed Shaping of $L(j\omega)$

The boundaries shown in Fig. 5.1 are used to illustrate the procedure with $\omega_h = 8$ rps, i.e., for all $\omega \geq 8$, L must lie to the right of the boundary marked V in Fig. 5.1 . It should be recognized that the phase at zero frequency is fixed at $0°$, or $-90°$, etc., according as to whether the system is Type Zero, or One, etc. This may not correspond to the optimum $L(j\omega)$, if there was no such constraint. However, the 'loss' due to this constraint can be made very small, because it is possible, at as low a frequency as desired, to have $L(j\omega)$ at the more favorable point, wherever it may happen to be. The practical limitation is the inconvenience of having poles and zeros very close to the origin. In Fig. 5.1, whatever may be the value of L at zero rps, it is easy to arrange that $L(j\ 0.5)$ have any desired value.

Consider the boundaries of Fig. 5.1 . Arbitrarily, let us try to achieve, say, -26 db at $\omega = 8$. Why is this impractical? Note that at $\omega = 4$, approximately - 10 db is needed for $|L|$. In order that $|L|$ decrease to - 26 db at $\omega = 8$, L must have an average slope of $-26 + 10 = -16$ db per octave over this range of frequencies

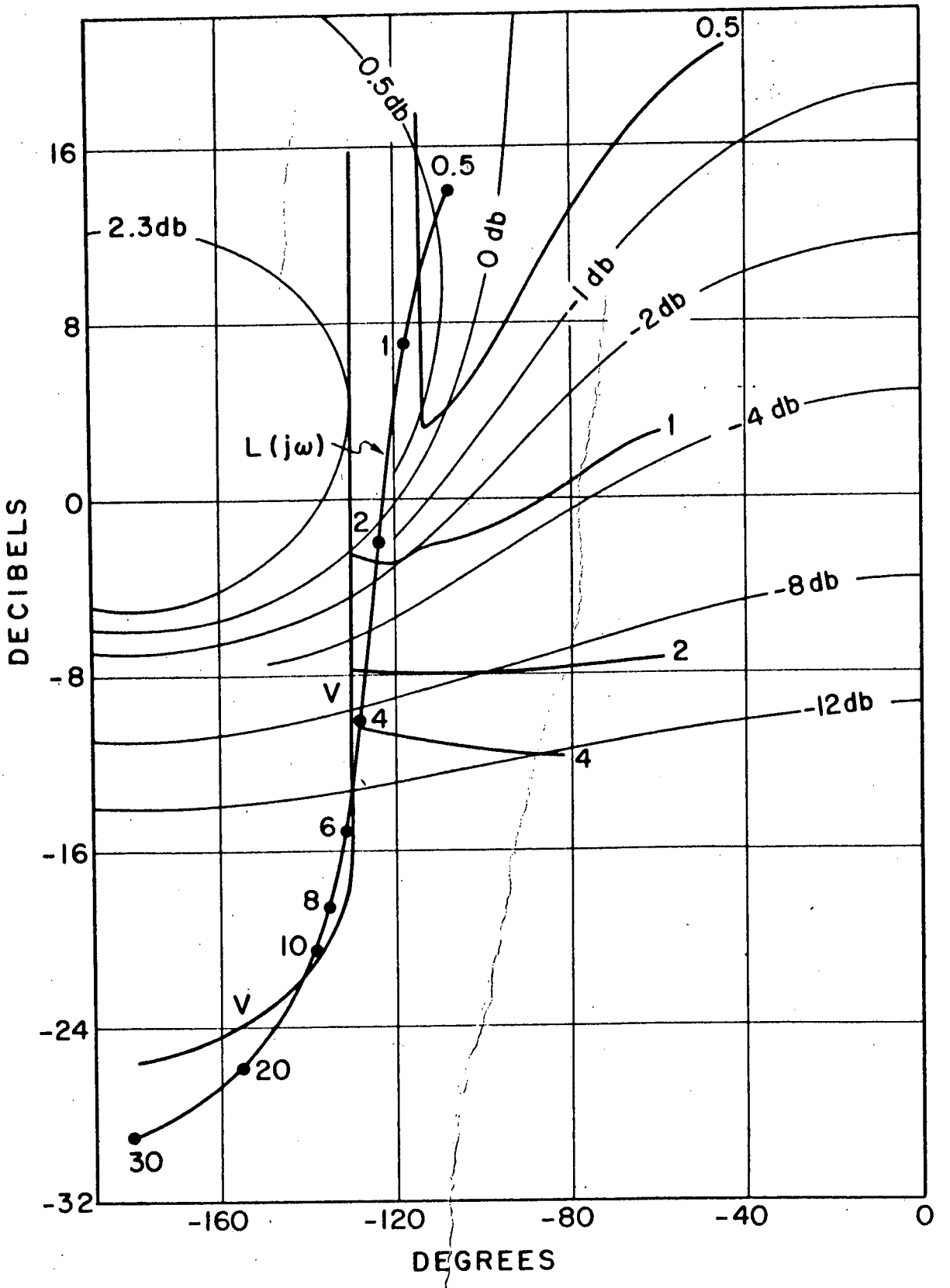

Fig. 5.1: Shaping of L(jω) - numerical example

(between $\omega = 4$ and $\omega = 8$) . But the average phase of L over this range is at best approximately $(-180 - 130)/2 = -155°$. With such a phase there is associated an average slope of $-155/180 \times 12 \approx -10$ db per octave, which is significantly less than the assumed - 16 db per octave. A value of -18 db for $|L|$ at $\omega = 8$ seems more reasonable. Let us check this value in the same manner. The average phase is, at best, now -130° (see Fig. 4.1), so the average slope of $|L|$ is $-130/180 \times 12 = -8\frac{2}{3}$ db/octave. If $|L(j4)| = -10$ db, then using the above slope, $|L(j8)| = -10 - 8\frac{2}{3} = -18\frac{2}{3}$, which is reasonably compatible with the assumption of -18 db at $\omega = 8$.

It is seen that the value of -10 db at $\omega = 4$ is a good starting point. It would be possible to use $|L(j4)| = -11$ db , providing $\angle L(j4) = -110°$. But then the average phase from $\omega = 4$ to $\omega = 8$ would only be $\frac{-110-130}{2} = -120°$, with an associated average slope of $\frac{-120}{180} \times 12 = -8$db/octave, so that $|L(j8)| \approx -11 - 8 = -19$, which is so close to $-18\frac{2}{3}$, as to make little difference. What of the other boundaries? What points on $\omega = 2$, 1 etc. should we aim for? On the $\omega = 2$ boundary, the -130° line is clearly the best, because the boundary is almost flat there. In any case, the average slope for $|L|$ near $\omega = 2$ is certainly such that if $|L(j4)| = -10$ db , then $|L(j2)|$ will be greater than -8 db, i.e., $L(j2)$ might as well be on V . Similarly, for $L(j)$. As for $L(j\ 0.5)$, we need only make certain that $\angle L(j\ 0.5)$ is close to -110° or so. Working backwards from $|L(j4)| = -10$ db, this means that $|L(j2)|$ will be approximately -1 db , $|L(j1)|$ approximately 7 db , and $|L(j\ 0.5)|$ approximately 15 db , providing we arrange to have approximately -130° phase for L from $\omega = 8$ to $\omega = 1$, and about -110° phase at $\omega = 0.5$.

How can the above phase values be simply obtained? An average phase of -130° may be obtained by alternating a lag corner frequency (lacf) with a lead corner frequency (lecf). Let $1+\alpha$ be the number of octaves under consideration, with a slope of -6 db/octave over one octave and a slope of

-12 db/octave over α octaves. Then the average phase lag is

$$(\angle L)_{av.} \approx \frac{-(6+\alpha 12)}{1+\alpha} \quad 180 \ , \tag{5.1}$$

which is to be -130° in the above example. Solving (5.1) for α gives $\alpha = 0.8$. Thus, if we allow a slope of -12 db/octave for one octave duration, we should allow a slope of -6 db/octave for 1/0.8 = 1.25 octaves.

The above results are applied to the example of Fig. 5.1, as follows. About -110° is desired at $\omega = 0.5$. This is a Type 1 system, so assign a lacf at ω_1, a lecf at $2\omega_1$, so that the asymptotic slope of -12 db/octave is over one octave, a lacf at $2^{1.25}(2\omega_1)$, so that the asymptotic slope of - 6 db/octabe is over 1.25 octaves, etc. Try various values of ω_1, until ω_1 is found such that the net result of an infinite series of the above leads to -110° phase at $\omega = 0.5$. To simplify the numbers, we used 2.5 instead of $2^{1.25} = 2.37$ and set $\omega_1 = 1$, which is a conservative choice. In accordance with the above procedure, the lacf at $\omega = 1$ is followed by a lecf at $\omega = 2$, a lacf at $\omega = (2.5)2 = 5$, and a lecf at (2)(5) = 10 rps. This procedure is halted at 10 rps, because near $\omega = 10$ we are permitted (see Fig. 5.1) a gradual decrease in phase. The level of $|L|$ is moved vertically until $|L(j4)| = -10$ db. The phase lag of the design, so far, is Curve A in Fig. 5.2.

The next lacf will be set at a somewhat higher frequency than would result from the above formula, because we wish to follow it with another two lacfs, in order to have a final asymptote of -24 db/octaves, corresponding to an excess of 4 poles over zeros for L(s). The situation at $\omega = 10$ is examined. At present $\angle L(j10) = -114°$, and from Fig. 5.1, it can be $\approx -140°$, if $|L(j10)| \gtrsim -26$ db. Hence 26° more lag

C.2

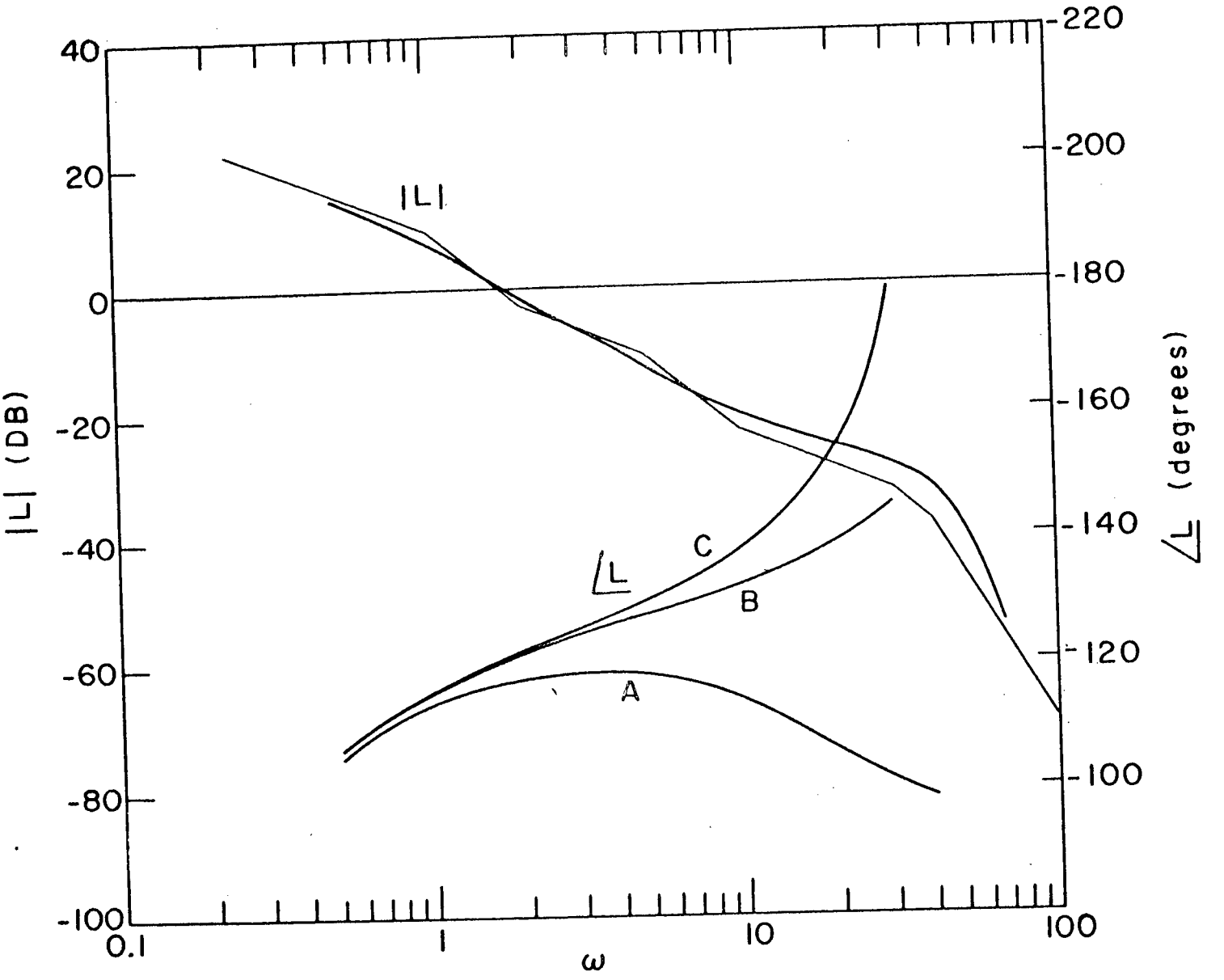

Fig. 5.2: Step-by-step shaping of $L(j\omega)$

is tolerable at $\omega = 10$. A lacf at $\omega = 30$ contributes $-18.5°$ at $\omega = 10$, leaving $7.5°$. The latter permits a complex pole pair at 4 rps, if its damping factor is 0.2 . The phase lag due to all poles and zeros, excepting the last complex pole pair, is given by curve B in Fig. 5.2, while the total phase lag is given by curve C . The resulting L is also sketched in Fig. 5.1 . The boundaries are slightly violated for $6 < \omega < 10$. More significantly, for $\omega > 12$, L could have more phase lag , which would permit its faster reduction.

The following relation[22] gives one an idea of the magnitude reduction available by increasing the phase lag:

$$\frac{2}{\pi}\int_0^\infty \theta \, d \ln \omega = -[\ln|L(0)| - \ln|L(\infty)|] \ . \qquad (5.2)$$

Compare two designs, in which $|L(0)|$ is the same in both, but in one region $\theta_2 < \theta_1$ by, say, an average of $20°$ over one octave. The difference between the two, for the left side of (5.2) is $\frac{2}{\pi}(\frac{20}{57.3}) \ln 2 = .154$ nepers $= 1.34$ db . Equation (5.2) is useful for estimating whether, in any particular problem, it is justifiable to seek to improve a tentative design. Thus, in Fig. 5.1, at $\omega = 0.5, 1, 2$ the phase lag could be increased by $6°$, $13°$, $6°$, respectively, so that the left side of (5.2) is increased in magnitude by about 1.7 db . However, most of the resulting increase in the difference between $\ln|L(0)|$ and $\ln|L(\infty)|$ would be due to an increase in $|L(0)|$. rather than a decrease in $|L(\infty)|$. The reason is that $|L(j4)|$ cannot be decreased, and since the increase in phase lag is in the frequency range less than 4 rps, the decrease in slope of $\ln|L(j\omega)|$ will occur primarily there. For this same reason, the increase in phase lag possible in the range $\omega > 12$ approximately, is more appealing, for it occurs in the

region $\omega > 4$, so most of the effect will be in the higher frequency range.

5.3 Loop Shaping by Working Backwards from $L(j\omega_h)$

A great deal of additional insight into the loop-shaping problem may be obtained by considering the following example in detail. Fig. 5.3 presents the contours and for the present purpose it doesn't matter how they were obtained. The boundary is a vertical line for all $\omega \geq 100$ rps . We are interested that $|L(j\omega_h)|$ be as small as possible. Let us try, at random, $|L(j100)| = -32$ db . Consider the $\omega = 10$ boundary, and try $L(j10) = -10$ db $\angle -110°$ (point Q in Fig. 5.3). Then, from 10 to 100 rps, the average slope of $|L| \approx -\frac{(110+140)\ 40}{2\ (180)} = -26.7$ db/decade, which is more than the $-32+10 = 22$ db needed. Hence, considering for the momeny only the $\omega = 10$ boundary, -32 db for $|L(j100)|$ is achievable. In fact, $|L(j100)| = -36.7$ db is achievable on this basis; perhaps an even smaller value by terminating on a lower portion of the $\omega = 10$ boundary. However, let us be content with the point Q_1 on the $\omega = 10$ boundary (because, in any case, as will soon be seen, other boundaries will not permit even this value to be attainable).

Consider the $\omega = 7$ boundary in Fig. 5.3 and see whether it is possible to reach this boundary from the desirable point Q_1 , (Q being assumed the best from the viewpoint of attaining $|L(j100)|$ min.) . The range from $\omega = 7$ to $\omega = 10$ covers 0.52 octaves. Try point R_1 ($0\ \angle -110°$) on the $\omega = 7$ boundary. It is impossible to achieve this, because the average slope magnitude is only $\frac{110}{180} \times 12 = 7\frac{1}{3}$ db per octave, operating over 0.52 octaves, which gives much less than the required 10 db from Q to R_1 . In this way, one finds it necessary to move down to point R_2 (-6.6 db $\angle -85°$) , for then the average slope of $-[\frac{110+85}{2}\ (\frac{12}{180})] \approx -6.5$ db/octave, over 0.52 octaves, gives the magnitude change of 3.4 db required between Q_1 and R_2 .

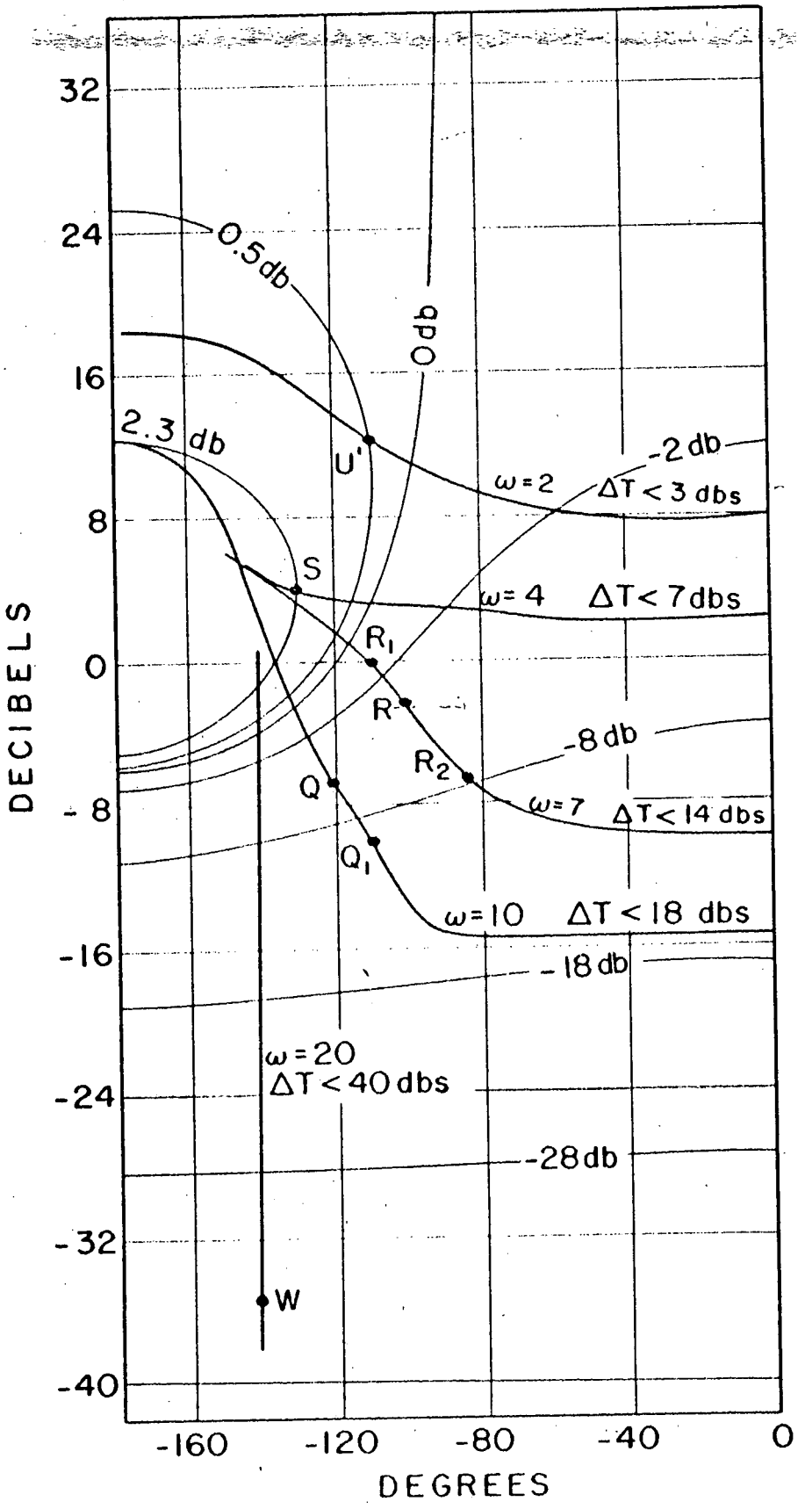

Fig. 5.3: Approximate loop shaping by working backwards from $L(j\omega_h)$

Next, consider the 4 rps boundary, and the transition from 4 to 7 rps, a range of 0.81 octaves. It is impossible to reach point R_2 from any point on the 4 rps boundary, as the smallest magnitude difference is more than 8 db, and the maximum average slope is less than 8 db/octave. It is therefore necessary to move up higher on the 7 rps boundary, which must therefore make it impossible to operate at Q_1, at 10 rps. The best one can do is to find the point closest to R_2 which permits transition to the 4 rps boundary, because this will then give the point closest to the unattainable Q_1. It is found that one must go all the way up to R ($\approx -2.3 \angle -102°$), with the corresponding point at S on the 4 rps boundary, and the point, Q on the 10 rps boundary, - 35.5 (point W) on the -140° line, which is the 100 rps boundary.

Next, consider the transition from the 2 rps boundary to point S. The point U ($12 \angle -110°$) is suitable, as the average slope of $-\left(\frac{110+130}{2}\right)\frac{180}{12} = -8$ db per octave, over one octave gives precisely the 8 db difference between U and S.

In this manner a compatible gain-phase trajectory for $L(j\omega)$ has been obtained, and which is a good approximation to the optimum. It is easier now to work by hand calculation, as it is known what to aim at. Also, it provides a good initial input trajectory for a computer program for computing L and finding its pole-zero pattern.

5.4 Design of Compensation in the Loop

It is hardly necessary to point out that the loop transmission, L, can always be written in the form $L = MP$, with M the compensation which must be inserted by the designer (in Fig. 1.1, $M = G$). Some set of plant parameters was chosen to obtain the boundaries of L. This resulting plant transfer function, at that set of plant parameters, could be denoted

by P_n . If so, the resulting $L(s)$ should be denoted by L_n , with $M(s) = L_n(s)/P_n(s)$. $M(s)$ will be independent of the particular choice of nominal plant parameters, i.e., of P_n . Since both $L_n(s)$ and $P_n(s)$ represent physically realizable transfer functions, so does $M(s)$.

CHAPTER 6

COMPLETION OF THE DESIGN

6.1 Design of Prefilter F

The work in the previous chapters, concentrating on the design of $L(s)$, guarantees that despite the specified bounds of plant ignorance, the change in $T(j\omega)$ remains within the allowable range. Thus, if $T(j\omega_1)$ is allowed to change from -3 db + 2 db, i.e., by a total of 5 db, then we can be certain only that the change in $|T(j\omega_1)|$ is by 5 db. However, the range of

$$\left|\frac{L(j\omega_1)}{1+L(j\omega_1)}\right|$$

may be from + 2 to + 7 db, or from any value K to (K + 5)db. It is therefore necessary to make use of the prefilter F of Fig. 1.1. Specifically, $|F(j\omega_1)|$ must be set at - 5 db, such that $|FL/(1+L)|_{\omega_1}$ ranges from - 3 to + 2 db.

The above, and the problems which may arise, are illustrated by the following numerical example.

6.2 Design Example

The plant transfer function is given by

$$P(s) = \frac{k}{s(s^2+S_p s + P_p)} \qquad (6.1)$$

with $1 \leq k \leq 1000$, and the complex pole pair of P ranging anywhere in the rectangle M, N, Q, U of Fig. 6.1a. The performance specifications require that the step response, characterizable by a dominant complex pole pair, be such that

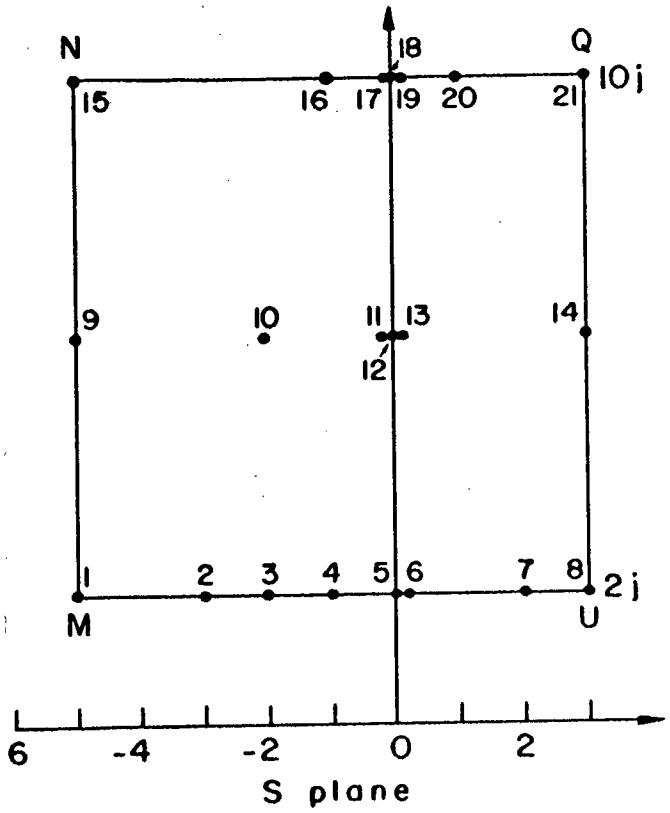

Fig. 6.1a: Range of complex pole pair of P(s)

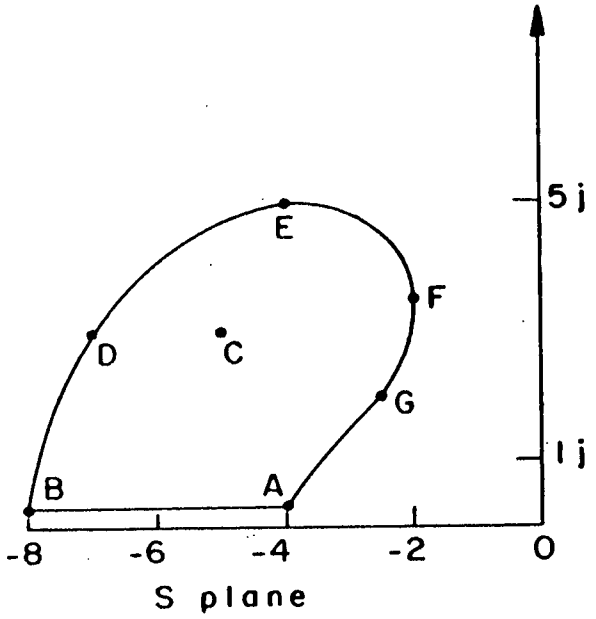

Fig. 6.1b: Acceptable range of complex pole pair of second-order model of T(s)

this complex pole pair lies within the region ABDEFG in the complex plane of Fig. 6.1b . This problem has been treated in the literature[8] by the Dominant Poles Method.

The first step was to translate the dominant-poles specifications of Fig. 6.1 into equivalent ones on $|T(j\omega)|$, the magnitude of the system transfer function frequency response. This step is at present handled, in general, as follows. Any simple model, such as a second-order one is used, and the range of model parameters found which satisfies the domain specifications. In this example this is already available, in Fig. 6.1b . The next step is to find the resulting range of variation of $|T(j\omega)|$. These are shown in Fig. 6.2a with the labels corresponding to those in Fig. 6.1b . [The reasoning is that magnitude control implicitly includes phase control; at least, it is worth trying. If not, then phase specifications can also be included and the design technique remains basically the same -- only the boundaries of permissible L will be affected.] Returning to Fig. 6.2a, it is important to broaden the permissible range of $|T(j\omega)|$ as much as possible, for clearly, this permits design by an $L(j\omega)$ of smaller bandwidth. To broaden the permissible range of $|T(j\omega)|$, one may proceed by trial and error, trying $|T(j\omega)|$ functions which progressively decrease faster as functions of frequency, until the time response specifications are intolerably violated. Similarly, one tries $|T(j\omega)|$ functions which progressively decrease more slowly versus ω , until again the time-domain specifications are intolerably violated. In this way, the significantly larger bounds shown in Fig. 6.2b were obtained.

The procedure of the previous chapters was then followed. Some of the plant templates are shown in Fig. 6.3 . Note that for $2 \leq \omega \leq 10$, they extend to infinity, because

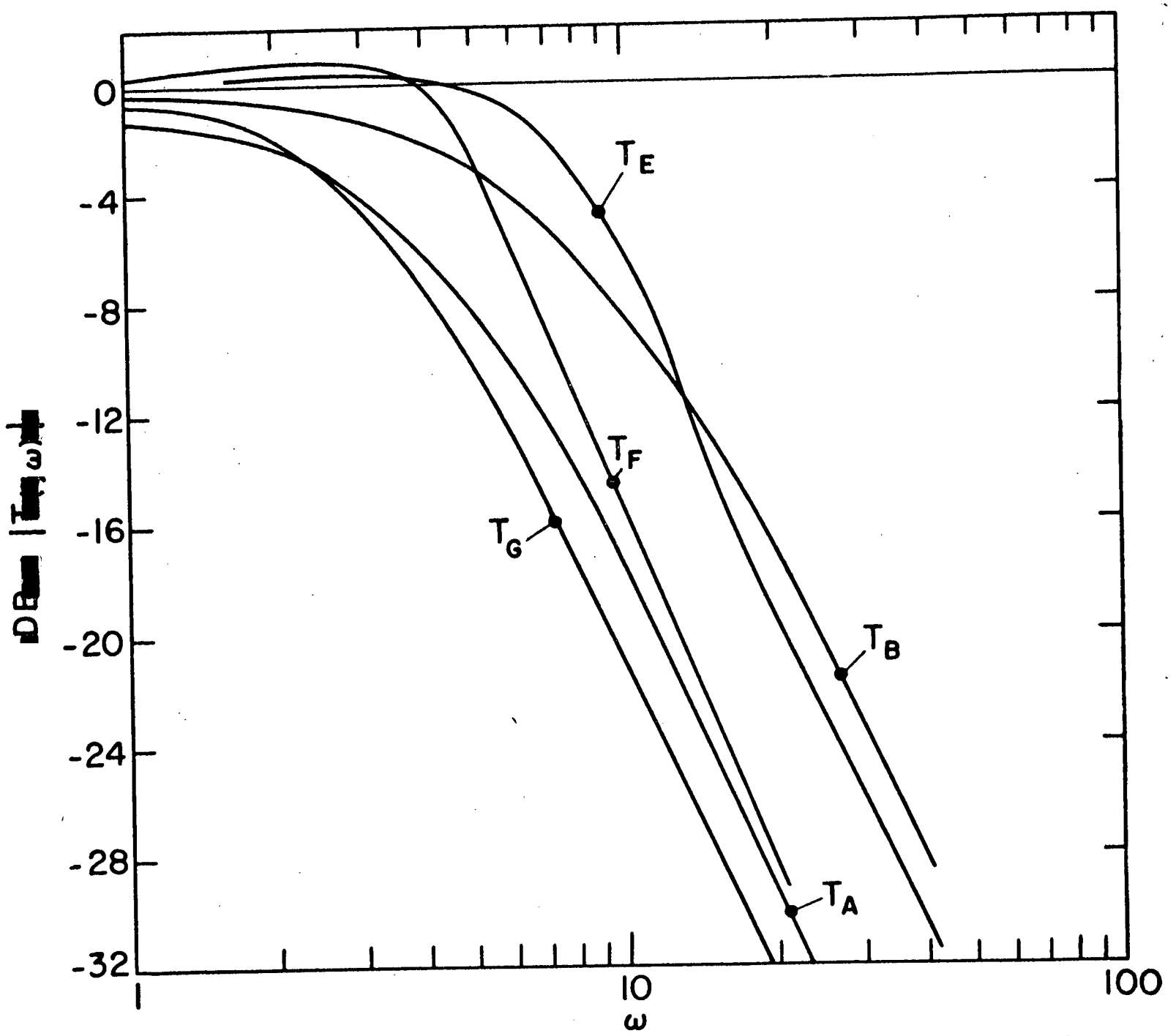

Fig. 6.2a: Frequency responses of $|T(j\omega)|$ corresponding to Fig. 6.1b

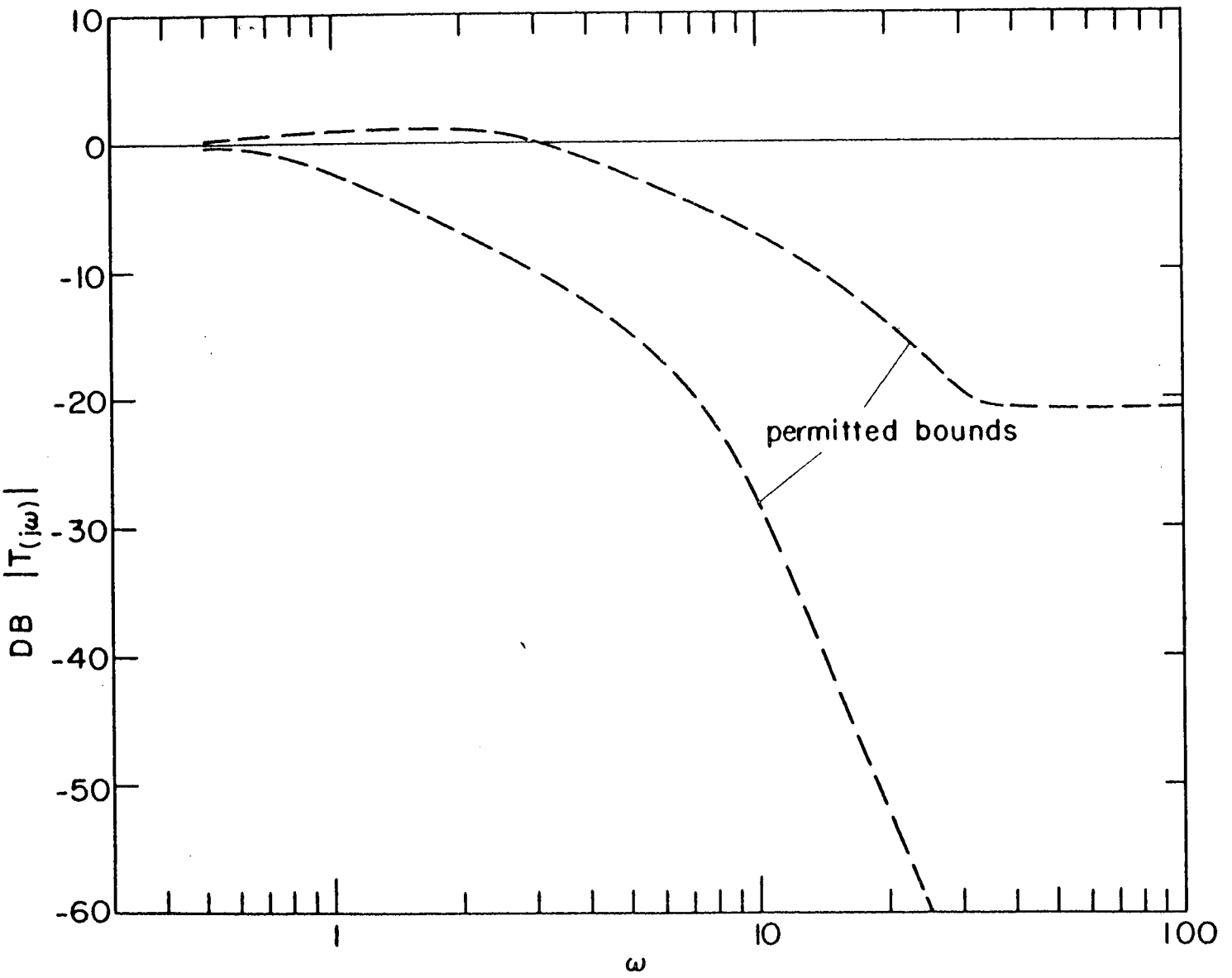

Fig. 6.2b: Larger $|T(j\omega)|$ bounds obtained by cut and try

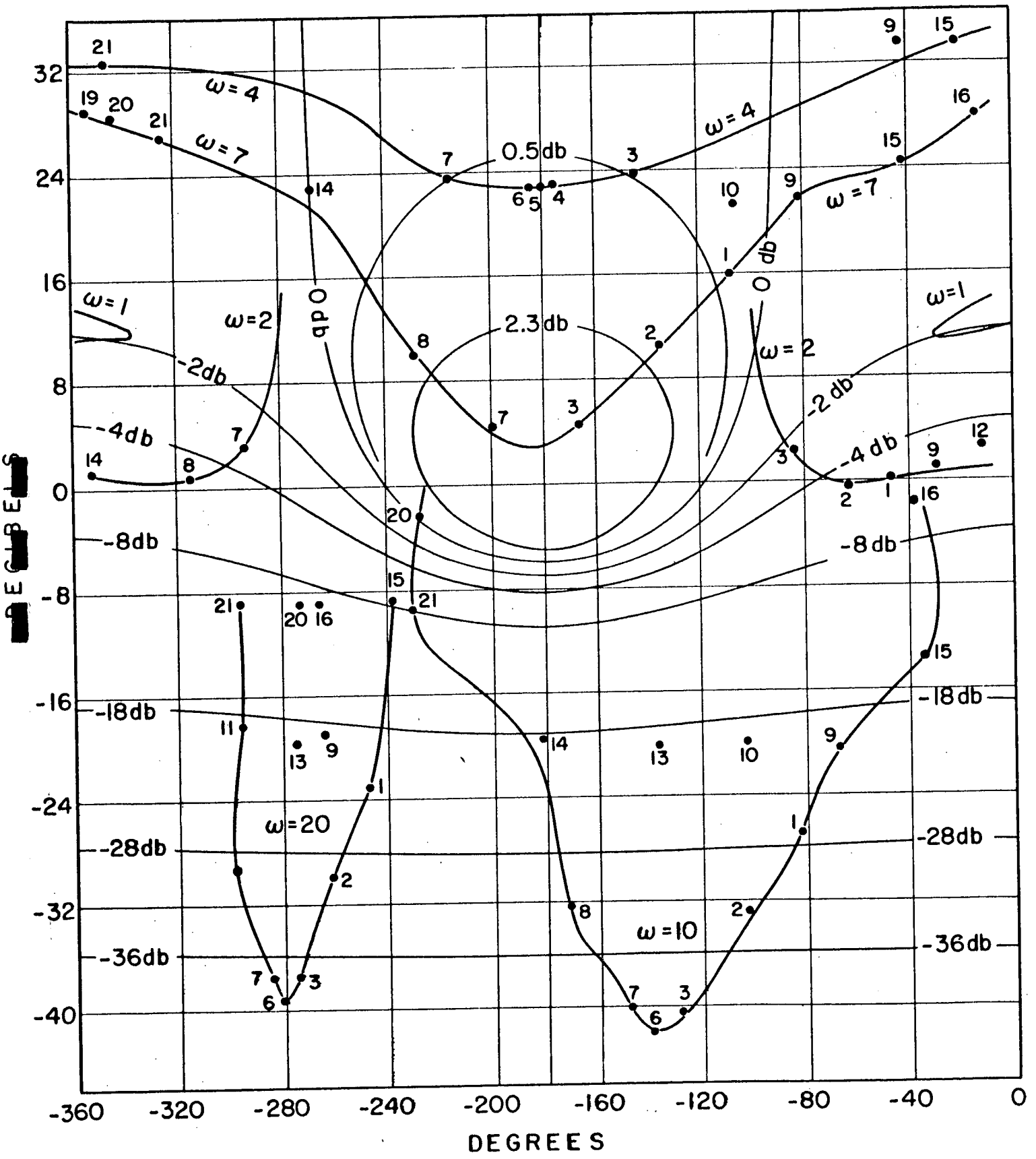

Fig. 6.3: Plant templates at various frequencies

this range is included in the plant pole range variation (see Fig. 6.1a). The resulting boundaries on L and several alternative designs of L are shown in Fig. 6.4 . These were all done by hand calculation. (Note the similarity with Fig. 5.3 . However, the boundaries at $\omega = 20, 40, 60$ were omitted in Fig. 5.3 , so the calculations there do not apply to Fig. 6.4 .) It is interesting to compare the four L_n's of Fig. 6.4 . The larger phase lag of L_{n1} results in a larger value of $[\ell n|L_n(0)| - \ell n|L_n(\infty)|]$, (recall Equation 5.2 and the discussion there). However, since this extra phase lag is in the low-frequency range, and the value at $\omega = 10$ is even higher than the rest, this difference means only a much larger $|L_{n1}(0)|$ than the rest. One should not make much of the small differences at $\omega = 100$ rps, because the design was performed by hand calculations, which do not permit very precise optimum design.

In any case, the resulting design leads to the changes in

$$\left|\frac{L(j\omega)}{1+L(j\omega)}\right| \triangleq |T'(j\omega)|$$

shown in Fig. 6.5a . Most of the responses lie outside the permitted boundaries. A prefilter F must be added and the requirements on $|F|$ are found, as explained in Sec. 6.1 . The results are shown in Fig. 6.5b . One may note that over some frequency range (up to about 3.3 rps) the boundaries are completely filled, but not for $\omega > 3.3$. This may seem surprising, because if $L(j\omega)$ lies precisely on its boundary at each frequency, then $\Delta\ell n|T(j\omega)|$ should cover precisely its entire permissible range. The reason for this discrepancy is that the boundaries have been restricted to some extent, due to the constraint on the disturbance response damping factor, as explained in Sec. 2.3 .

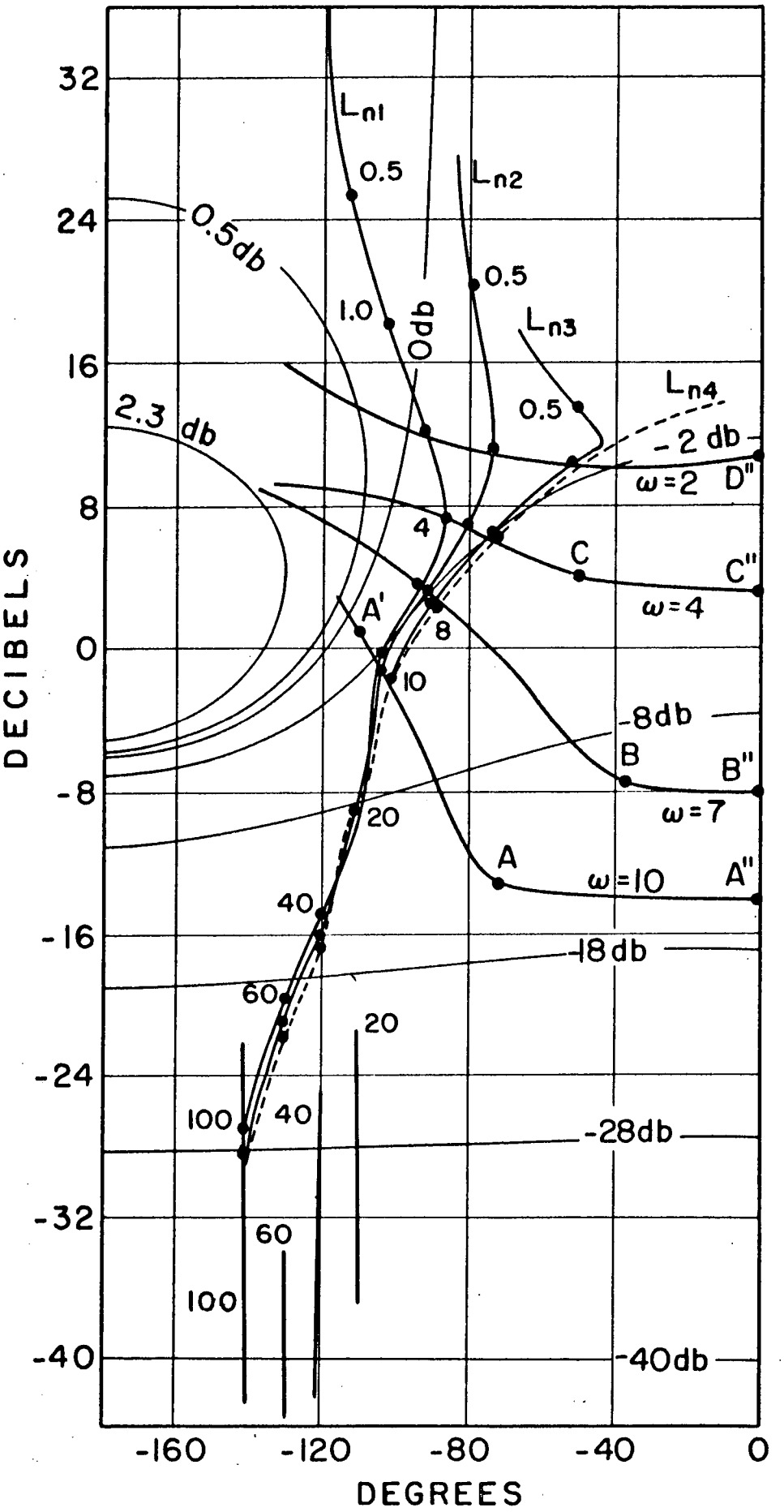

Fig. 6.4: Boundaries of $L(j\omega)$ and some $L(j\omega)$ designs

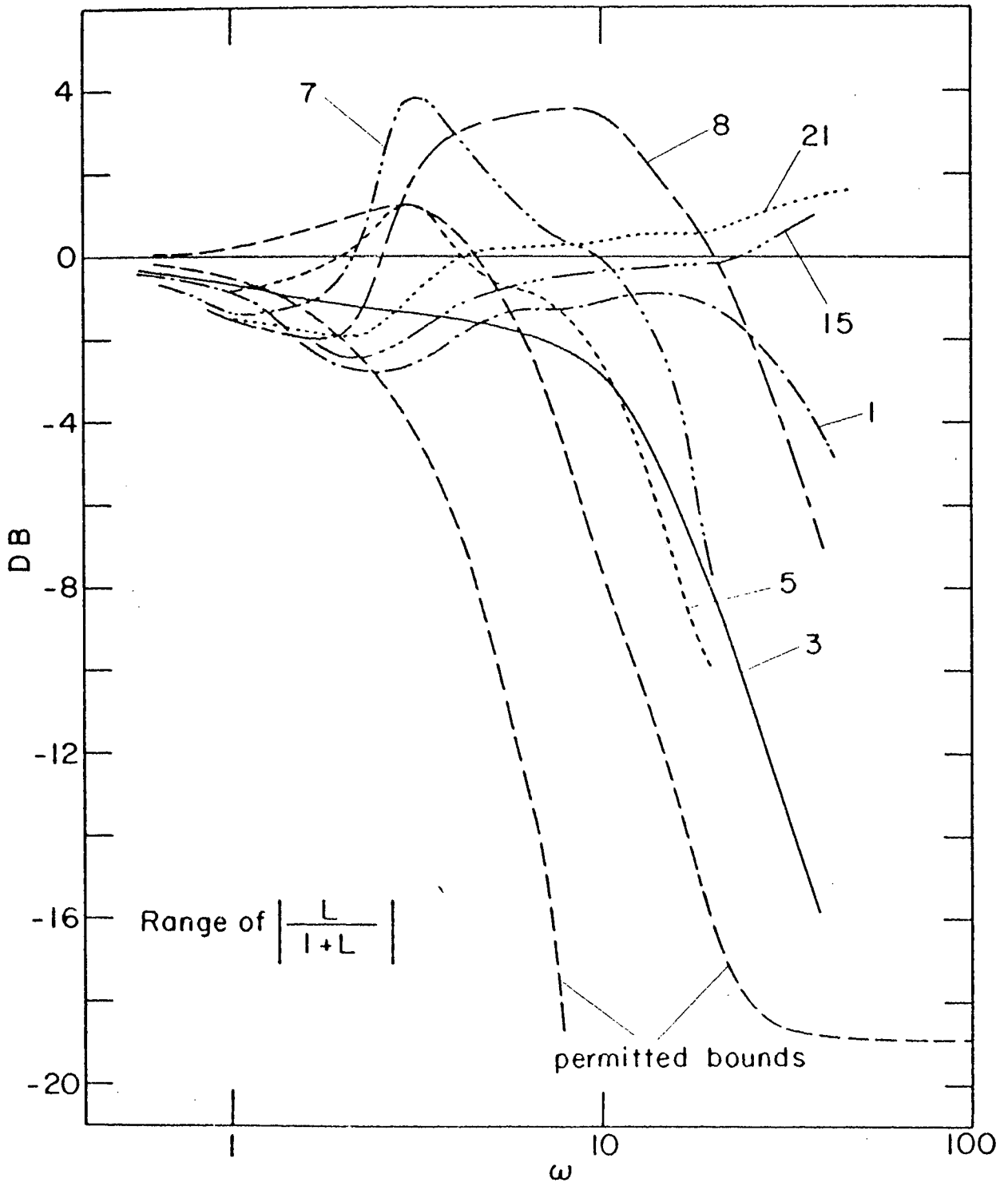

Fig. 6.5a: Design of first prefilter

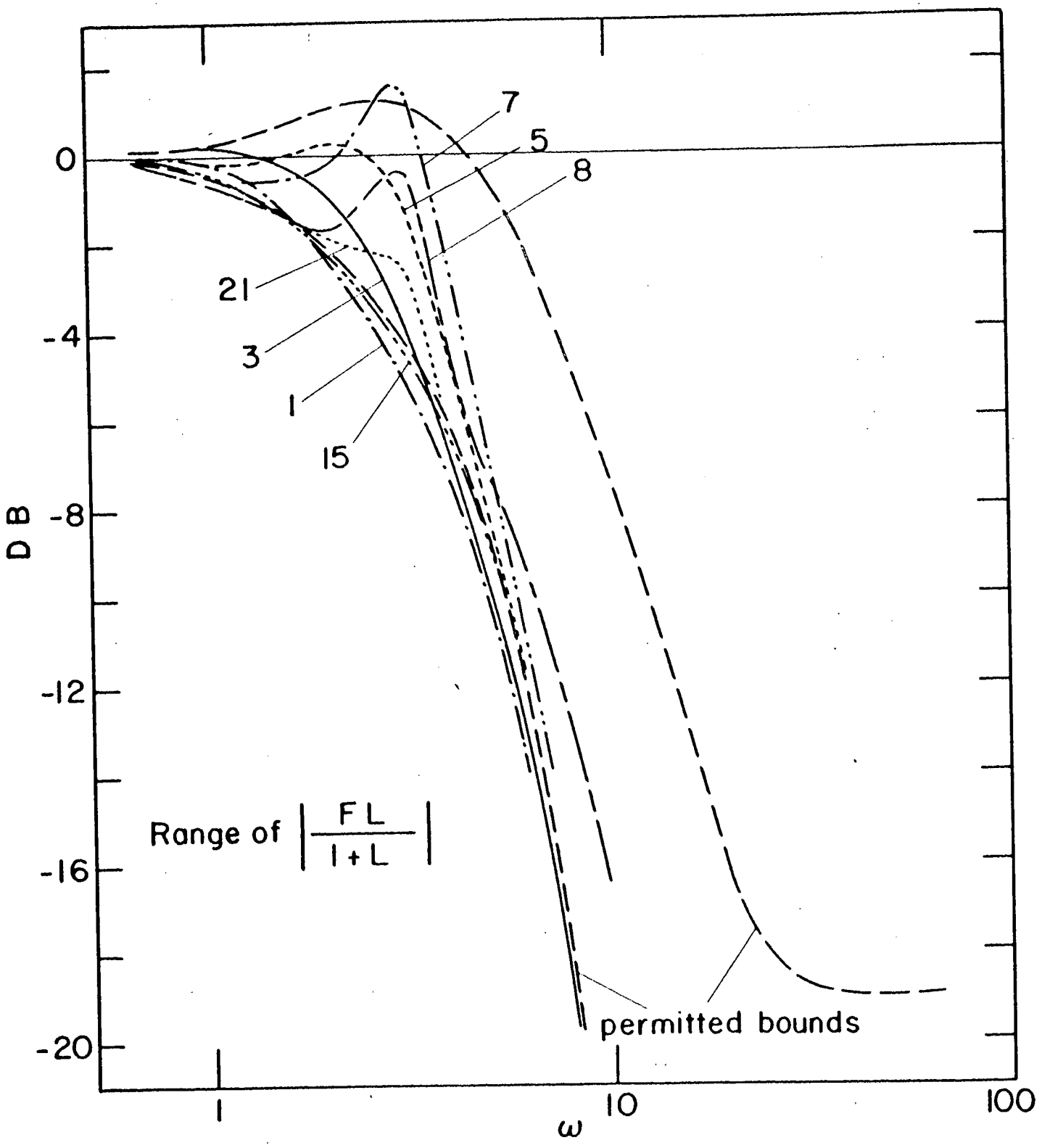

Fig. 6.5b: Design of first prefilter

The step responses resulting from Fig. 6.5(b) are shown in Fig. 6.6 . These responses fall within the time response bounds corresponding to the complex pole range of Fig. 6.1b. However, there are some time responses whose behavior, as a function of time, may not be acceptable. The reference is to Curve 8, in which the first overshoot is below the final value. The corresponding frequency response marked '8' in Fig. 6.5(b) has a minimum followed by a peak which does not reach the $|T(0)|$ reference. We shall refer to this as the "wobbling problem". (It is interesting to note that reflection of the $|T(j\omega)|$ frequency response about the y axis at $\omega = 0$, gives a roughly qualitative picture of the system step response. This is especially true of the 'wobbling' phenomenon.) The wobbling problem will be next considered.

6.3 The Wobbling Problem

Case 8 in Fig. 6.5b is a good example of a 'wobble' in $|T(j\omega)|$. Evidently, at a low frequency, (2 rps), case 8 must be at the low end of the template of $P(j2)$, see Fig. 6.3, template marked $\omega = 2$. When this template is positioned to find the boundary of acceptable $L(j2)$, Case 8 lies near the low extreme of $|T(j2)|$. On the other hand, at $\omega = 3$, if the template of $P(j3)$ is calculated, it is found that Case 8 lies near the top of the template, towards the left side, which means that it will be near the high extreme of $|T(j3)|$. The occurrence of a wobble of this type may therefore be predicted when there are some plant conditions which exhibit this kind of behavior.

How can the 'wobble' in the frequencu response be eliminated? The simplest but least economical way is to increase the level of $|L|$ for all ω . The corrective

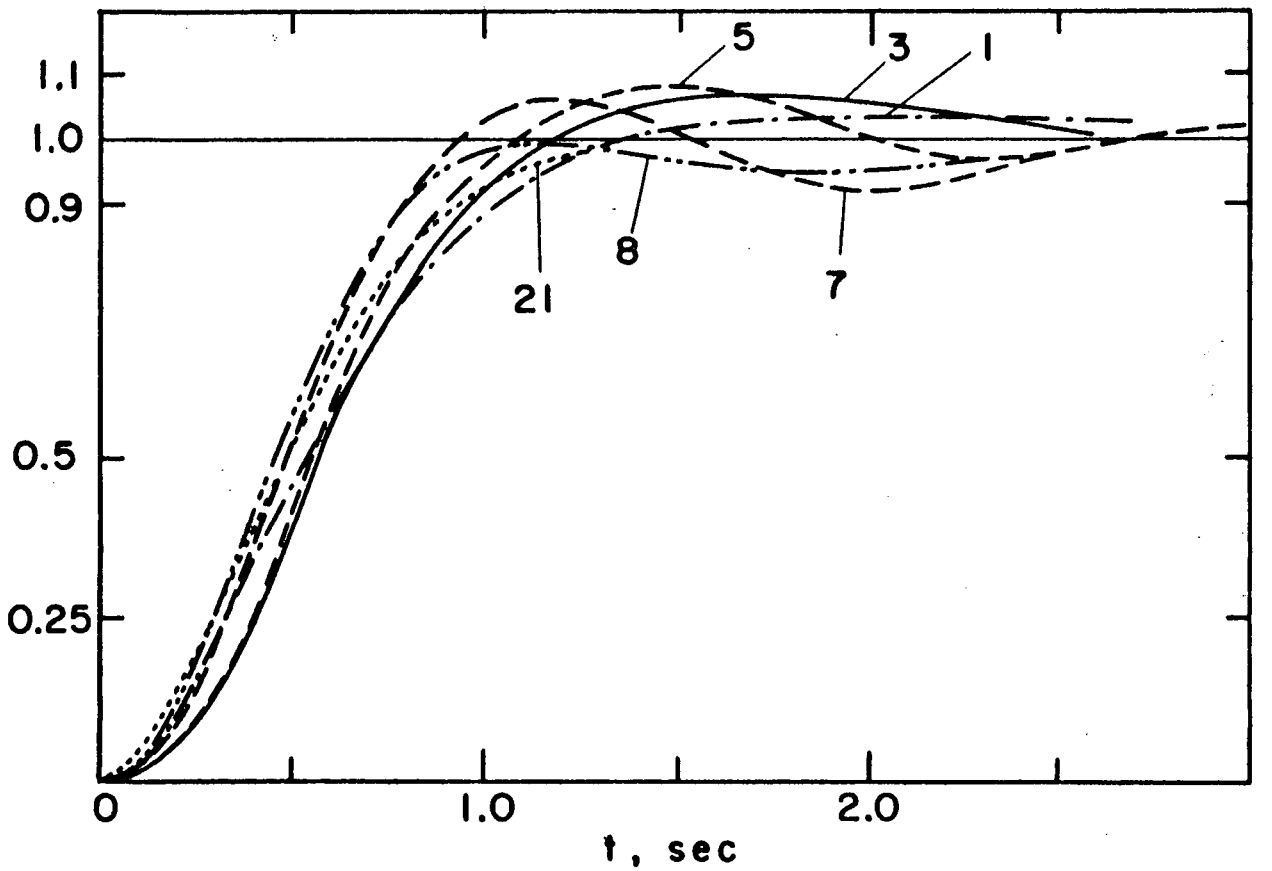

Fig. 6.6: Step responses for $T(j\omega)$ of Fig. 6.5b

effect is as follows -- see Fig. 6.7 . At $\omega = 2$, the position of $L_8(j2)$ is, say, in the neighborhood of Q , i.e., in the low end, while at $\omega = 3$, $L_8(j3)$ is say, at U , in the high end. Increase of $|L|$ at the same phase improves matters at both frequencies. It decreases $|T|$ at $\omega = 3$, and increases it at $\omega = 2$, both effects helping to straighten out the wobble. This method was used in the above design example, increasing $|L|$ by 2 db . The new $|FL/(1+L)|$ values are shown in Fig. 6.8a, and their step responses are sketched in Fig. 6.8b .

It is certainly possible to eliminate the wobble in a more economical manner, i.e., with a smaller increase of $|L|$ at high frequencies. The two principal frequencies of the wobble, i.e., the minimum and maximum points, which were at $\omega = 2,3$ for Case 8 in Fig. 6.5b, are considered. Fig. 6.9a is used to present the argument, with extreme wobbling for Condition 1, between ω_1 and ω_2 . Suppose L is changed at ω_1 such that $|T_1|$ is increased and $|T_2|$ is lowered, from points A_1, A_2 to points B_1 , B_2 , respectively. This by itself alleviates the wobbling problem in two ways. First, the difference in level between $T_1(\omega_1)$ and $T_1(\omega_2)$ is reduced by $\log B_1 - \log A_1 \triangleq \delta_1$. Second, it is possible to improve matters by modifying the prefilter (F) value at ω_1 . Let the new $|F(j\omega_1)|$ be larger than the old, by the amount $\log A_2 - \log B_2 \triangleq \delta_2$. The result is to restore $|T_2(j\omega_1)|$ back to the position A_2 , and to increase $|T_1(j\omega_1)|$ precisely by the amount δ_2 . Thus, the total improvement is $\delta_1 + \delta_2$. The same two effects occur at ω_2 if a change of L at ω_2 causes a decrease in $|T_1(j\omega_2)$ and an increase in $|T_3(j\omega_2)|$.

There remain the following questions to be answered. How much of the improvement should be assigned to ω_1 ,

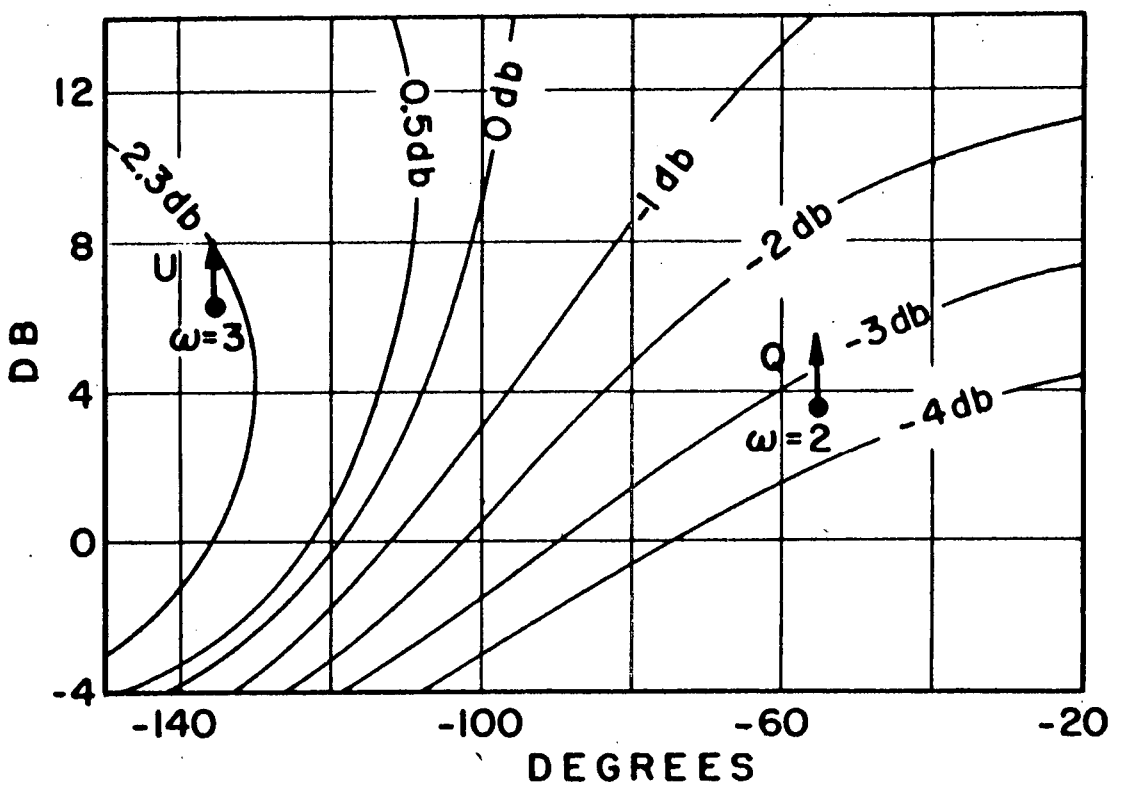

Fig. 6.7: Effect of increase of |L| on wobble

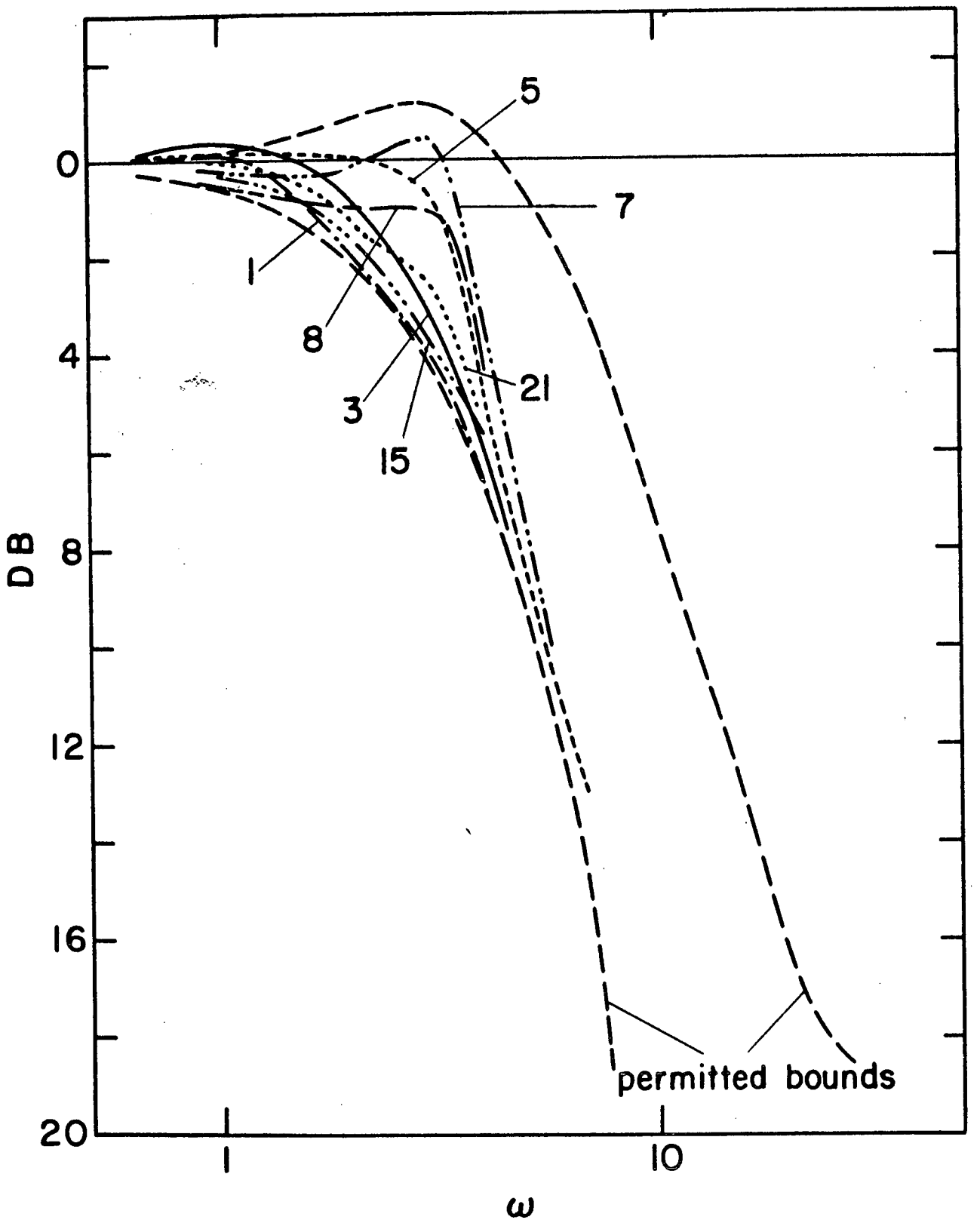

Fig. 6.8a: $|T(j\omega)|$ when $|L|$ increased by 2 db

and how much to ω_2 ? Whatever the amount assigned to either, how is it to be attained, i.e., how should L be changed at that frequency? At any frequency one can find the net gradient of $|T|$, as follows. Consider Fig. 6.9b, whose points A_1, A_2 correspond to the equivalent points in Fig. 6.9a . The gradient of $|T|$ is, of course, normal to the contours of constant $|T|$. The solid arrows are drawn in the desired direction in each case, i.e., at A_2 it is desirable to decrease $|T_2|$, while at A_1 , it is desirable to increase $|T_1|$. Let the length of the arrows be assumed proportional to the gradient magnitudes. Then the net gradient is the vector sum of the two arrows and gives the optimum direction for decreasing $|T|$ with least change in $|L|$, at that specific frequency. Superficially, it would seem that one could thus find the net gradients at each of ω_1 , ω_2 and assign the burden of correction to each, in proportion to their net magnitudes. But the matter is not that simple, because a change in $|L|$ is associated to some extent with a change in $\angle L$ and the change cannot be local only. For example, suppose $\Delta L = 2 \text{ db} \angle 30°$ is desired at $\omega_1 < \omega_2$. This can be achieved by means of a suitable [23] 'finite line segment' properly placed (Fig. 6.9c). The phase lead exists for only a part of the frequency range, while the magnitude change persists for all $\omega > \omega_x$ and its benefits are therefore available for all $\omega > \omega_x$. Hence, if the ω_2 of Fig. 6.9a is not much larger than ω_1 , it is certainly worthwhile maintaining the level of the correction (denoted by G) to ω_2 . Also, it is clearly better to use Fig. 6.9c , rather than increase the level of $|L|$ by the same amount for all ω , because Fig. 6.9c permits the desired phase lead to be simultaneously obtained, and so obtain a correction lined up with the net gradient

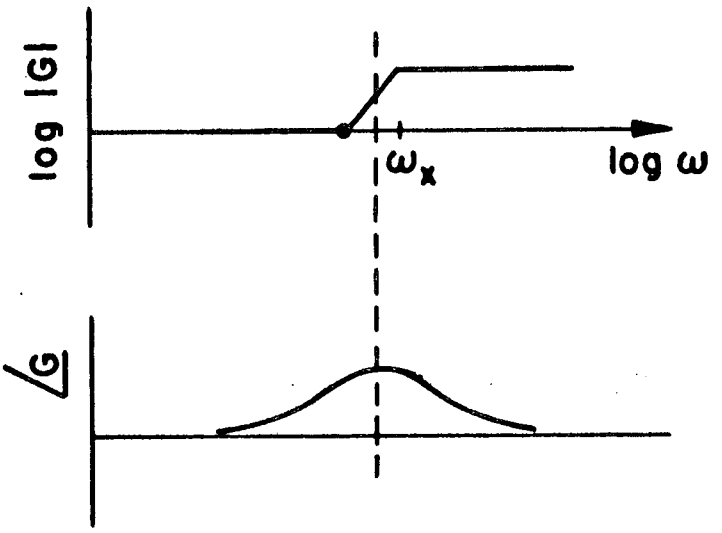

Fig. 6.9c: Wobbling problem considerations

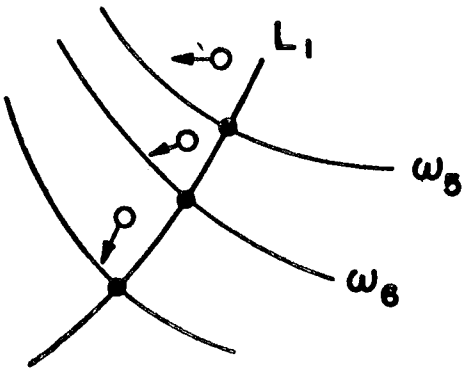

Fig. 6.9d: Wobbling problem considerations

calculated for the point ω_1 . It is possible to make additional adjustments at ω_2 , to try thereby to achieve a correction there, also lined up with the gradient.

The net 'loss' to the system, in the form of larger $|L|$ at high frequencies, is available from Equation (5.2) , when $|L(0)|$ is maintained at its former value. It is, therefore, desirable at higher frequencies where correction is not necessary, to reduce $|G|$ back to zero db . If that is possible, them there will be an associated phase lag which will cancel the phase lead in Fig. 6.9c, and by Equation (5.2), there will then be no net loss. This is impossible to do completely, if our original design for L was indeed an optimum design. But it is at least possible to partially do so (see Fig. 6.9d). Let L_1 be the original optimum loop transmission which resulted in the wobbling problem. Let the circles represent the result of the correction which eliminated the wobbling. For simplicity, it is assumed ω_5 is sufficiently large so that the phase of the correction G is back to zero at ω_5 , so the circles are vertically above the former points on L_1 . A negative 'finite line-segment' if introduced here, would have the effect indicated by the arrows. It could, at least theoretically, be shaped optimally to reduce the 'loss' as much as possible. It is certainly better to do this than to allow the correction, i.e., this higher level of $|L|$, to stand as is over this higher frequency range where it is not needed.

CHAPTER 7

CONCLUSIONS

7.1 Unfinished Work

This report has presented a procedure for design of two-degree-of-freedom feedback systems with parameter ignorance and specified acceptable time-domain performance bounds. One of the attractive features of the technique is its transparency. At every point the designer understands the basic conflicts between the desiderata, especially the relation between the loop bandwidth and its effect on the system response variations. Another advantage is in the speed of the design. Once the designer understands the method, he can design a problem such as the one described in Chapter 6 in about ten working hours, if he has computer programs for evaluating time from frequency response and vice versa.

There are several important uncompleted parts. One is the study of the optimum $L(j\omega)$ for the general case. A second is the wobbling problem. A third is the translation of time response bounds to frequency response bounds. In addition, it would be very desirable to automate the design steps as much as possible. The automation of the calculation of the templates of $P(j\omega)$ is easy and has been done. The determination of the boundaries of $L(j\omega)$ on the Nichols chart is relatively easy to do by hand and is probably best left that way. But it would certainly be desirable to have a computer program for finding $L(j\omega)$, or at least to polish it up after the initial approximation by the methods of Chapter 5.

7.2 Application to Disturbance Attenuation

The same technique may be applied to the problem of disturbance attenuation accompanied by plant parameter ignorance. Consider the three disturbances of Fig. 7.1, one

by one.

$$T_{D_3} = \frac{C}{D_3} = \frac{1}{1+L} \tag{7.1}$$

with

$$L = GP_1P_2 \quad . \tag{7.2}$$

Let $\ell = \frac{1}{L}$ and then

$$T_{D_3} = \frac{C}{D_3} = \frac{\ell}{1+\ell} \tag{7.3a}$$

$$\ell n\left|\frac{C}{D_3}\right| = \ell n\left|\frac{\ell}{1+\ell}\right| \tag{7.3b}$$

The rotation of the Nichols chart by 180° is equivalent to the transformation $L = 1/\ell$. Hence, the Nichols chart may be so used for T_{D_3} . Templates of $P = P_1P_2$ are found in the same manner as before and so are boundaries of $\ell(j\omega)$ to satisfy given frequency response specifications on T_{D_3} , etc.

Consider

$$T_{D_1} = \frac{C}{D_1} = \frac{P}{1+PG} = \frac{P_0}{\frac{P_0}{P} + P_0G} = \frac{P_0}{\frac{P_0}{P} + L_0} \tag{7.3}$$

where P_0 is any nominal plant transfer function. It may be more convenient to work in the complex plane, rather than in the Nichols chart. At any given frequency, the range of P_0/P may be found. Suppose it is as shown in Fig. 7.2 at $\omega = \omega_1$. Suppose also that $-L_0(j\omega_1)$ at point A_1 is under consideration. Then

$$T_{D_1} = \frac{P_0(j\omega_1)}{AB} \tag{7.4}$$

where B may range anywhere inside or on $\frac{P_0}{P}(j\omega)$. One may then find the boundary of the $-L_0(j\omega_1)$ which satisfies the

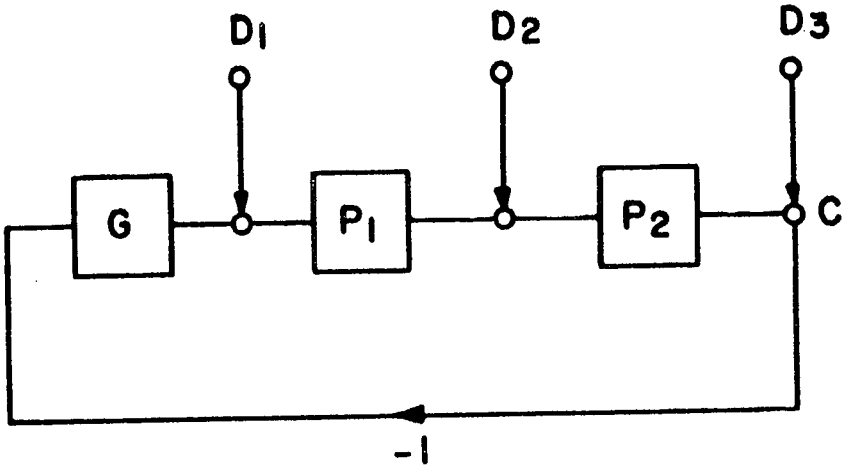

Fig. 7.1: System with three kinds of disturbances

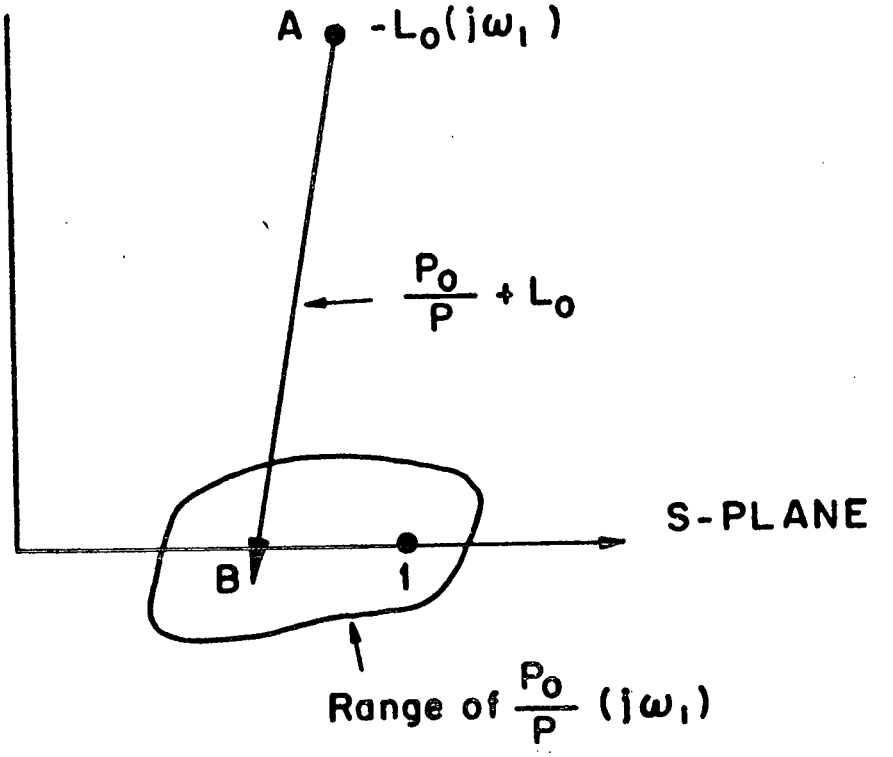

Fig. 7.2: Design technique for D_1

frequency response specifications on T_{D_1} . The balance of the design is straightforward.

Finally, consider

$$T_{D_2} = \frac{C}{D_2} = \frac{P_2}{1 + P_1P_2G} = \frac{P_{20}\,\frac{P_{10}}{P_1}}{\frac{P_{10}P_{20}}{P_1P_2} + L_0} \quad . \tag{7.5}$$

The boundaries of $\gamma_1 \triangleq \frac{P_{10}}{P_1}$, $\frac{P_{10}}{P_1}\,\frac{P_{20}}{P_2} \triangleq \gamma_{12}$ are obtained and sketched as in Fig. 7.3 . The region A of γ_1 maps into the larger region A' of γ_{12} , B into B' and parts of A',B' may overlap. This is all at some specific frequency ω_1 . From Equation (7.5)

$$T_{D_2} = \frac{P_{20}\gamma_1}{MN} \tag{7.6}$$

When the region A in γ_1 is considered, then the appropriate range of N , in Fig. 7.3, is A' etc. In this way boundaries of acceptable $-L_0(j\omega_1)$ may be obtained and the design continued by the methods of this report. Alternatively, one may work on the Nichols chart by writing

$$T_{D_2} = \frac{P_1P_2\,\frac{1}{P_1}}{1 + P_1P_2G} = \frac{L/P_1}{1+L} \tag{7.7a}$$

so

$$\ell n|T_{D_2}| = \ell n\left|\frac{L}{1+L}\right| + \ell n|P_1| \quad . \tag{7.7b}$$

When the template of P is manipulated on the Nichols chart, it is necessary to consider also the template of P_1 , in a manner equivalent to Fig. 7.3 .

Finally, if there are specifications on both the system response to commands, and its response to disturbances, it is possible by the means described to find the resulting boundaries of $L(j\omega)$ for each separately, and then take the worst of both, such that both sets of requirements are satisfied.

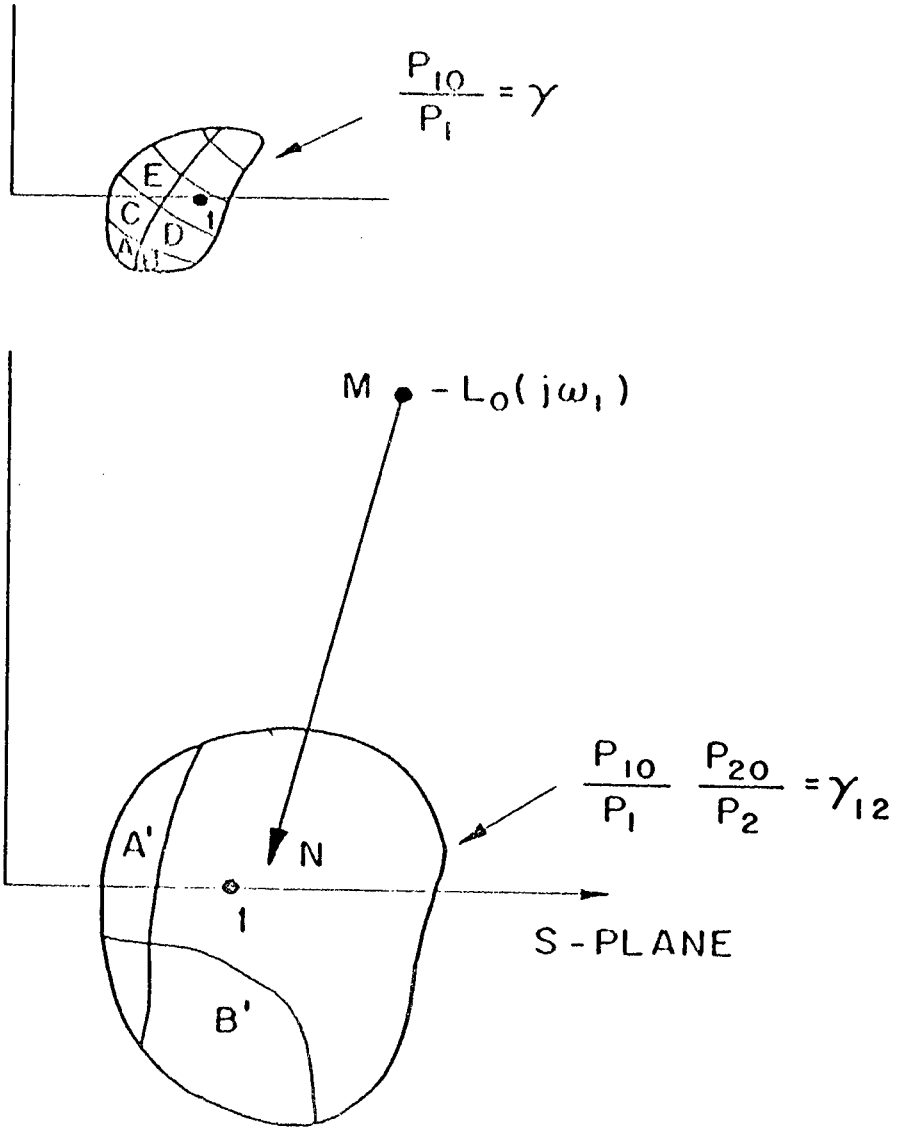

Fig. 7.3: Design technique for D_2

REFERENCES

1. I. Horowitz, Synthesis of Feedback Systems, Academic Press, 1963, pp. 170, 239, 246.

2. Ibid, pp. 332, 351.

3. Ibid, pp. 441-452.

4. Ibid, Secs. 5.9, 6.14, p. 373.

5. P. Fleischer, Optimum Design of Passive-Adaptive Linear Feedback Systems with Varying Plants, IRE Trans. on Automatic Control, Vol. AC-7, March 1962, pp. 117-128.

6. D. E. Olson and I. Horowitz, Design of Dominant-Type Control Systems with Large Parameter Ignorance, International Journal of Control, Vol. 11, 1970, pp. 545-554.

7. H. Z. Lewis, Computer-Aided Design of Feedback Control Systems with Plant Parameter Variations, Department of Electrical Engineering Research Report, University of Colorado, June 30, 1970.

8. I. Horowitz, Optimum Linear Adaptive Design of Dominant-Type Systems with Large Parameter Variations, I.E.E.E. Trans. on Automatic Control, Vol. AC-14, June 1969, pp. 261-269.

9. I. Horowitz, Fundamental Theory of Automatic Linear Feedback Control Systems, IRE Trans. on Automatic Control, Vol. AC-4, December 1959, pp. 5-19.

10. Reference 1, pp. 267-285.

11. I. Horowitz, Linear Adaptive Flight Control for Reentry Vehicles, I.E.E.E. Trans. on Automatic Control, Vol. AC-9, January 1964, pp. 90-97.

12. N. Oda, Frequency Response Approach to Design of Adaptive Control Systems via Model of Specifications, M.E.E. Thesis, Department of Electrical Engineering, University of Colorado, June 1969.

13. Reference 1, pp. 313-4.

14. H. W. Bode, Network Analysis and Feedback Amplifier Design, D. Van Nostrand, 1945. Chapters 14, 15.

15. Reference 1, pp. 307-319; Equations (7.5, 2) .

16. Reference 14, p. 302, Formula V(a) .

17. Reference 14, p. 302, Formula VI(a) .

18. Z. Nehari, Conformal Mapping, First edition, McGraw-Hill, 1952, pp. 141 et seq.

19. Reference 18, p. 143.

20. Reference 14, pp. 328-9.

21. Reference 1, p. 319.

22. Reference 14, p. 286; Reference 1, p. 317.

23. Reference 14, p. 338; Reference 1, p. 316.